# Czech Technical University in Prague

## Faculty of Mechanical Engineering

Department of Automotive, Combustion Engine and Railway Engineering

# Master´s thesis

## Multi-speed Gearbox for Passenger EV

Supervisors:

Ing. Michal Jasný

Satrio Wicaksono ST, M.Eng., Ph.D.

2021                                                      Bc. Maroš Kováč

# MASTER'S THESIS ASSIGNMENT

## I. Personal and study details

| | | | |
|---|---|---|---|
| Student's name: | **Kováč Maroš** | Personal ID number: | **452803** |

Faculty / Institute: **Faculty of Mechanical Engineering**

Department / Institute: **Department of Automotive, Combustion Engine and Railway Engineering**

Study program: **Master of Automotive Engineering**

Branch of study: **Advanced Powertrains**

## II. Master's thesis details

Master's thesis title in English:

**Multi-speed Gearbox for Passenger EV**

Master's thesis title in Czech:

**Vícestupňová převodovka pro elektrický osobní automobil**

Guidelines:

1) Summarize the usage of single and multi-speed gearboxes used in electric passenger cars.
2) Propose a powertrain layout for chosen type of electric car with a range of at least 250 km. The layout must be suitable for usage of single and multi-speed gearboxes.
3) Perform a vehicle driving simulation using one of the standardized driving cycles and compare the energy balance using a one-, two- and three-speed gearbox. Select suitable vehicle parameters.
4) Choose one of the multi-speed gearbox variants and create a CAD model focusing on the internal gear mechanism. Perform basic strength calculations and prepare production drawing of one part according to the agreement with the supervisor.
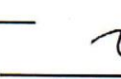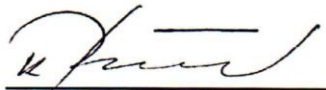
Bibliography / sources:

SAE Papers, CTI Papers, Simulink Help, GT Suite Help

Name and workplace of master's thesis supervisor:

**Ing. Michal Jasný,    Department of Automotive, Combustion Engine and Railway Engineering,    FME**

Name and workplace of second master's thesis supervisor or consultant:

Date of master's thesis assignment: **30.10.2020**        Deadline for master's thesis submission: **06.01.2021**

Assignment valid until: _____

| Ing. Michal Jasný | doc. Ing. Oldřich Vítek, Ph.D. | prof. Ing. Michael Valášek, DrSc. |
|---|---|---|
| Supervisor's signature | Head of department's signature | Dean's signature |

## III. Assignment receipt

The student acknowledges that the master's thesis is an individual work. The student must produce his thesis without the assistance of others, with the exception of provided consultations. Within the master's thesis, the author must state the names of consultants and include a list of references.

_____29.11.2020_____        _____Kováč_____
Date of assignment receipt            Student's signature

# ANNOTATION:

| | |
|---|---|
| **Author:** | Bc. Maroš Kováč |
| **Title in English:** | Multi-speed Gearbox for Passenger EV |
| **Title in Czech:** | Vícestupňová převodovka pro elektrický osobný automobil |
| **Academic year:** | 2020/2021 |
| **Study Program:** | Master of Automotive Engineering |
| **Major:** | Advanced Powertrains |
| **Department, Faculty:** | Department of Automotive, Combustion Engine and Railway Engineering, Faculty of Mechanical Engineering (CTU in Prague)<br>Faculty of Mechanical and Aerospace Engineering (ITB) |
| **Supervisors:** | Ing. Michal Jasný (CTU)<br>Satrio Wicaksono ST, M.Eng., Ph.D. (ITB) |

| | |
|---|---|
| **Abstract:** | This thesis consists of a review of electric vehicle gearboxes, driving simulation of the vehicle equipped with the single and multi-speed gearboxes and a proposal of a multi-speed gearbox for the passenger EV |

| | |
|---|---|
| **Keywords:** | Multi-speed gearbox, electric vehicle, helical gear, software simulation |
| **Number of pages:** | 86 |
| **Number of figures:** | 50 |
| **Number of tables:** | 41 |

## DECLARATION

I hereby declare that I have completed this thesis independently and that I have listed all literature and publications used in accordance with the methodological guidelines about adhering to ethical principles in the preparation of the final thesis.

In Prague, 6th of January, 2021                    ……………………………

Signature

## ACKNOWLEDGMENT:

# TABLE OF CONTENT

# INTRODUCTION

Nowadays, we increasingly encounter the term electric vehicle (the vehicle that uses an electric motor as a power source). The first electric vehicle (EV) was manufactured in 1884. Nevertheless, the popularity of EV did not significantly increase until the turn of the millennium. This change is caused by various reasons such as limited amount of fossil fuels connected with the increasing gas prices, environmental and legislative vehicle emission restrictions and recent improvements in the battery and electric motor technologies.

However, as the demand for EVs increases, so do the demands of customers, which force manufacturers to improve their vehicles. The main requirements include an improvement of the vehicle´s performance and an increase in the range of the car per single battery charge along with the charging speed. To meet these demands, the EV powertrains, are subject to continuous research and improvements. One of the main components of the powertrain, which participates on the effective usage of the electric energy is a gearbox. A properly designed gearbox can directly improve vehicle performance and lower the electric energy consumption, thus increasing the range of the vehicle. This presumption made this thesis, which aims to propose a multi – speed gearbox, possible.

In the first part of the thesis, I describe individual components of the electric propulsion systems and summarize the usage of single and multi-speed gearboxes used in electric passenger cars currently available on the market.

In the second, practical, part of the thesis, I first propose a powertrain layout which is suitable for usage of a single and multi-speed gearboxes. Subsequently, I choose the electric vehicle, equip it with three different types of gearbox and perform a driving simulation on the Worldwide Harmonized Light Vehicle Test Cycle in order to compare energy balance using one-, two- and three-speed gearbox.

The last part includes the design procedure of the multi speed gearbox. The proposal process is supplemented with basic geometry and strength calculations necessary to ensure proper function of the gearbox. Eventually, for visualization purposes I create the CAD model of the gearbox focusing on the internal gear mechanism. The appendix of the thesis contains additional gear strength calculations as well as a production drawing of the gearbox output shaft and a drawing of the gearbox cross-section.

# THEORETICAL PART

## 1.1 ELECTRIC PROPULSION SYSTEMS

The term propulsion system comprises all devices and units which are responsible for the transfer of power to driven wheels of the car. The electric car´s propulsion system contains (similarly to a vehicle with internal combustion engine) the engine (electric motor), shafts, gearbox and final drive / differential. The electric vehicle is entirely powered by electric motors. The energy, necessary for running the car, is stored in batteries and through the inventor it is sent to the electric motor (EM). Electrical energy is delivered to the batteries from the electrical power network using various types of chargers or by recuperation of energy during braking. From the electric motor, the power is transferred via shafts and optionally a clutch in some types of multi speed gearboxes, into the transmission. The function of this device is to reduce high engine's RPM to desired wheel's RPM and simultaneously to multiply the motor's torque by means of gears. Power is subsequently sent to the differential gear that transmits it to the wheels.

There are various configurations of the electric vehicle propulsion system. These configurations are shown in Figure 1. (a) - (f).
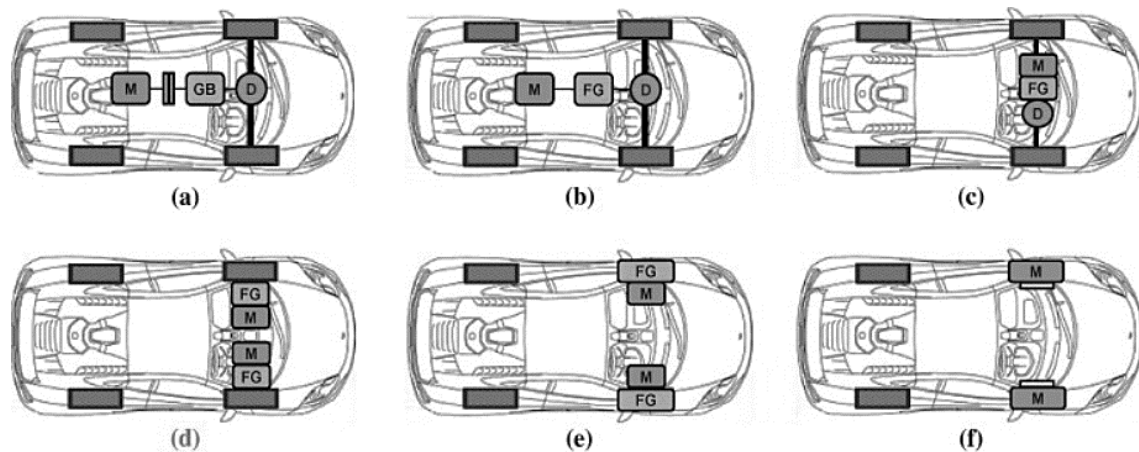


*Figure 1 – Configuration of electrical powertrain, M – electric motor, GB – multi speed gearbox, FG – fixed gear gearbox, D – Differential [8]*

In the configuration shown on Figure 1(a), the motor is connected to driving wheels through the clutch, multi speed gear box and differential. Different EV configuration is obtained by replacing the gearbox with fixed gearing or planetary gearbox hence removing the clutch (weight and size of the system is reduced) as shown in Figure 1(b). Figure 1(c) shows the integration of motor, gearbox and differential into a single unit.

Figure 1(d) shows the configuration of the propulsion system with two electric motors and two gearboxes, which allows to omit final drive. In the layout shown in Figure 1(e, f) the gearboxes/electric motors are mounted inside the wheels.

## 1.2 GEARBOXES

A gearbox is a machine that uses gears and gear trains to provide conversion of RPM and torque between input and output units. In application in a vehicle with internal combustion engine, a gearbox is necessary to adapt the relatively small range of effective RPMs and torque to a significantly higher range of required vehicle velocity and tractive forces. Various gear ratios allow the operation of a combustion engine in arbitrary RPM regardless of vehicle velocity. Another function of a gearbox is to allow reverse drive or in some applications to activate parking brake when a vehicle is stationary, to prevent it from motion [20].

The purpose of a gearbox in electric vehicles is different. In contrast to the internal combustion engine, an electric motor can produce a maximal torque from zero RPMs. However, the efficiency of the EM is not constant and it varies from the speed and load that will be discussed in the chapter 1.3. In high RPM, the maximum torque slightly decreases. Due to this reason electric motor speed does not have to be adjusted as it is in conventional cars; thus, a multiple speed gearbox is not necessary for EV. The gearbox in EV provides a reduction of the relatively high RPM of electric motor to lower RPM of a car's wheels.

### 1.2.1 TYPES OF TRANSMISSIONS

Transmissions can be divided into different groups according to various criteria from which I chose the following three:

According to the method of gear ratio change:

- **Shifting without power interruption** - gear ratio is changed continuously without interruption of torque flow. The ratios can be engaged under load. For example: conventional automatic transmissions, dual clutch transmissions.
- **Continuously variable transmissions without power interruption** – gear ratio shifting does not occur in steps but it differs continuously. For example – hydrodynamic converter, friction gears

- **Shifting with power interruption** – gear ratio is changed stepwise, torque flow is interrupted while gears are being engaged and disengaged. Efficiency is higher, able to transfer higher loads. [20]

According to the type of individual gear engagement:

- **Manual transmissions** – a driver controls gear changes via gear lever and clutch pedal.

- **Semi-automatic transmissions** – gear change is control by a driver with help of an auxiliary device (hydrodynamic/pneumatic force, spring, electromagnetic force).

- **Automatic transmissions** - gear change occurs automatically without the driver's intervention. It is controlled by transmission control unit, which evaluates riding conditions and engages optimal gear.[4]

According to construction:

- **Gear wheel transmissions**

  - **Single stage countershaft transmission** – torque for each gear is transferred via single gear pair

  - **Two stage countershaft transmission** - torque for each gear is transferred via 2 gear pairs. This arrangement contains intermediate shaft that carries gears but does not transfer the primary drive of the gearbox either in or out of the gearbox.

  - **Planetary transmission** – torque is transferred via epicyclic gear set with gears in constant mesh. Individual gears are changed by adjustment of speed of gear wheels, hence gear change under full load is possible.

- Transmissions with electrical gears

- Hydrostatic, friction, belt transmissions [20]

## 1.2.2 TRANSMISSIONS IN ELECTRIC VEHICLE APPLICATIONS

As mentioned in chapter above, electric vehicles does not require multi-gear transmission to satisfy the characteristics of internal combustion engine. According to 1.2.2.1-1.2.2.3 nowadays almost every mass produced EV is equipped with single speed fixed gear ratio transmission, where torque is transferred via gear mesh. This layout is popular due to its simplicity, small dimensions and no need for clutch mechanism.

However latest trends indicate, that using multi-gear gearbox leads to better performance of electric drive in terms of top speed and range (electric energy consumption).[6] It is caused by the characteristics of an electric motor, which indicate that at high RPM the maximum torque and efficiency of the motor decreases. By engaging lower gear ratio, speed of the electric motor is reduced, hence torque is increased. First gear generates higher torque necessary during acceleration while other gears allow vehicle to achieve higher top speed and better efficiency. [6]

## 1.2.2.1   SINGLE SPEED COUNTERSHAFT (LAYSHAFT) TRANSMISSION

Countershaft gearbox consists of three shafts – input (driving), intermediate and output (driven). Torque enters the transmission via input shaft. Through first pair of gears, torque is transferred to the intermediate shaft and subsequently through a second pair of gears to the output shaft. The number of gear pairs located on the intermediate shaft determines the number of gears the gearbox has. All gear pairs are in constant mesh. Two layouts for layshaft transmissions are commonly used: [20]

- **Coaxial layshaft transmission**

Input and output shaft for this arrangement are mounted coaxially, as we can see from Figure 2 below. Usually the size of this configuration is compact and none of the dimensions is significantly higher than the other ones. Due to the position of gears on the layshaft, this shaft is loaded by relatively high bending moments. Among mass produced electric vehicles, Chevrolet Bolt EV and BMW i3 are equipped with this type of gearbox. [1] [21]
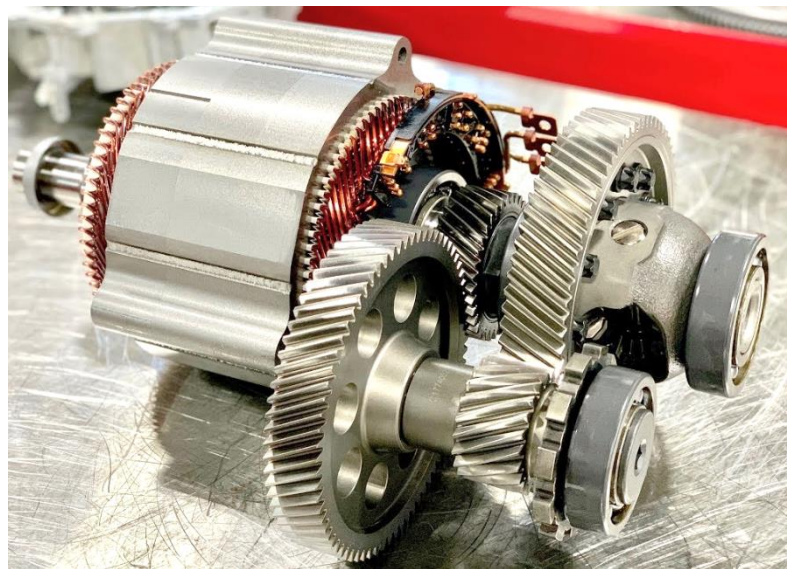


*Figure 2 - Coaxial layshaft transmission – Chevrolet Bolt EV [1]*

- **Parallel layshaft transmission**

Each shaft in this configuration is mounted parallel. Axes of these shafts can lay in different planes to achieve a more compact size of the gearbox. Otherwise the length of transmission increases. Parallel layshaft transmission is used more than a coaxial one. Nissan Leaf, VW e – Golf, Tesla Model X and S are equipped with this gearbox. [2],[22]
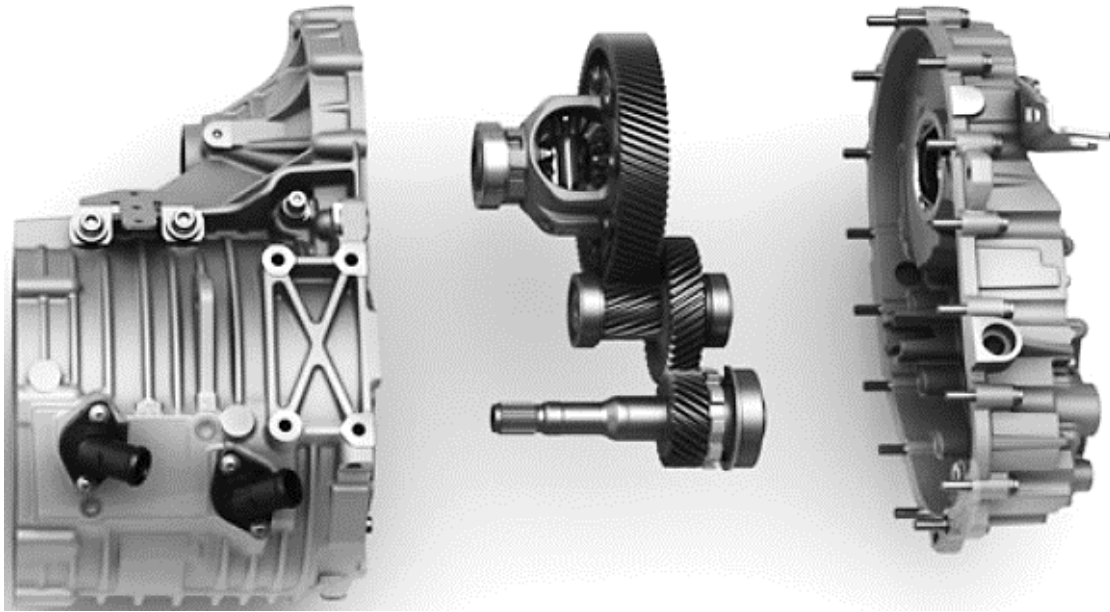


*Figure 3– parallel layshaft transmission – Volkswagen e – Golf [2]*

## 1.2.2.2 SINGLE SPEED PLANETARY TRANSMISSION

The planetary gear set consists of three main components – a sun gear, planet gears which are supported by the planet carrier, and a ring gear. In this system pinions connected by a planet carrier rotate around another gear (sun gear) in a manner similar to the revolution of the planets around the sun. Planetary gear set can be arranged in many ways to offer required parameters.

The biggest advantage over layshaft system is that gears can be engaged under full load without interruption of the torque flow. However, in contemporary EV applications, planetary gearboxes operate as a single speed fixed gear ratio systems, thus the mentioned advantage is not utilized. Due to the single speed arrangement, this type of gearbox is less complicated and compact compared to multi – gear planetary transmissions. Torque, which usually enters the transmission through the sun gear is transferred to several pinions. Hence, the force distribution is better than in layshaft transmissions, which allows to use gears with a smaller modulus. This configuration causes absence of radial force loads on all bearings except satellite bearings. [3][20]

Planetary transmissions are popular in modern electric vehicles. Car manufacturers prefer this configuration because of its compact dimensions and convenient force distribution. Electric SUVs such as Jaguar I-Pace and Audi E – TRON are equipped with this gearbox. The last one mentioned uses the combination of both planetary and spur gear.
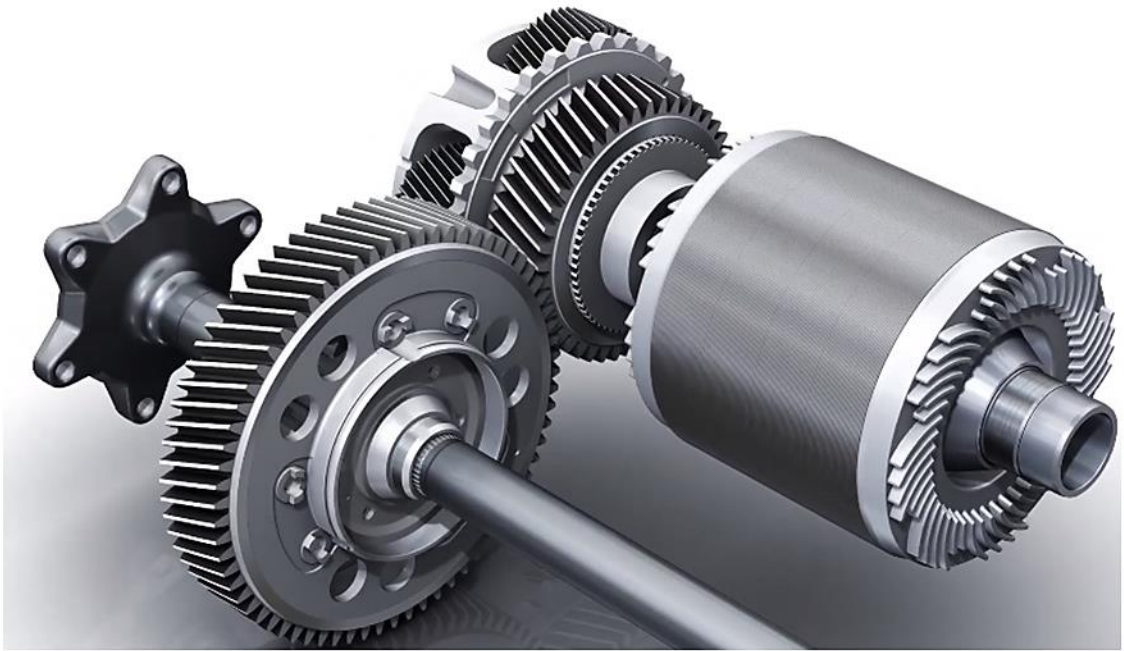


*Figure 4 - A combination of the planetary and the spur gear transmission – Audi E – TRON [5]*

### 1.2.2.3   TWO SPEED TRANSMISSIONS

Nowadays, almost every mass produced electric vehicle is equipped with a single speed fixed gear ratio transmission. One of the biggest benefits of these gearboxes is their simplicity, compact dimensions and no need for a clutch and complicated gear changing mechanisms. When the fixed gear ratio is designed precisely the electric motor can deliver satisfactory performance in terms of acceleration and top speed.

Latest trends and research indicate that electric vehicles fitted out with multi speed gearboxes can improve the vehicle's performance by helping optimize both low-speed acceleration and top-end speed. [6] By employing multiple transmission gear ratios, the electric motor is able to work in an effective range of RPM, hence the overall propulsion system can be made to operate more efficiently throughout the vehicle operating range. Simulation results highlight potential increases in WLTP drive cycle range. By integrating the electric motor with a multi-speed transmission, the motor torque

requirement reduces motor volume and mass. This enables greater dimensional flexibility. [6]

Among the mass production electric vehicles, there is only one that is fitted out with multi speed transmission – Porsche Taycan. Porsche uses two electric motors for the front and rear axle, thus it is equipped with 2 gearboxes. The front axle electric motor is paired with single speed fixed gear coaxial layshaft transmission. Rear axle gearbox comprises one planetary gear set and two pairs of spur gear as can be seen from Figure 5 and Figure 6
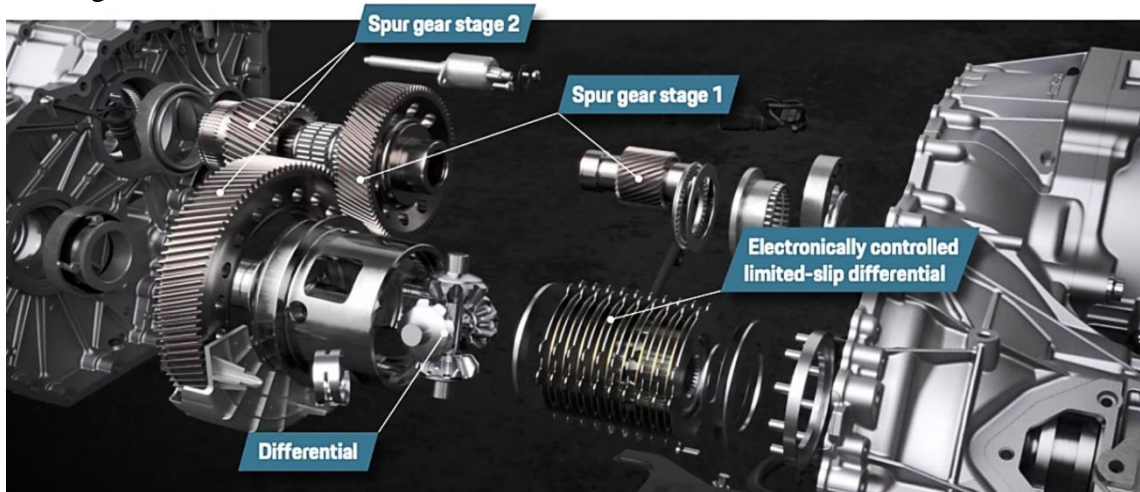


*Figure 5 - Multi speed transmission – Porsche Taycan [7]*
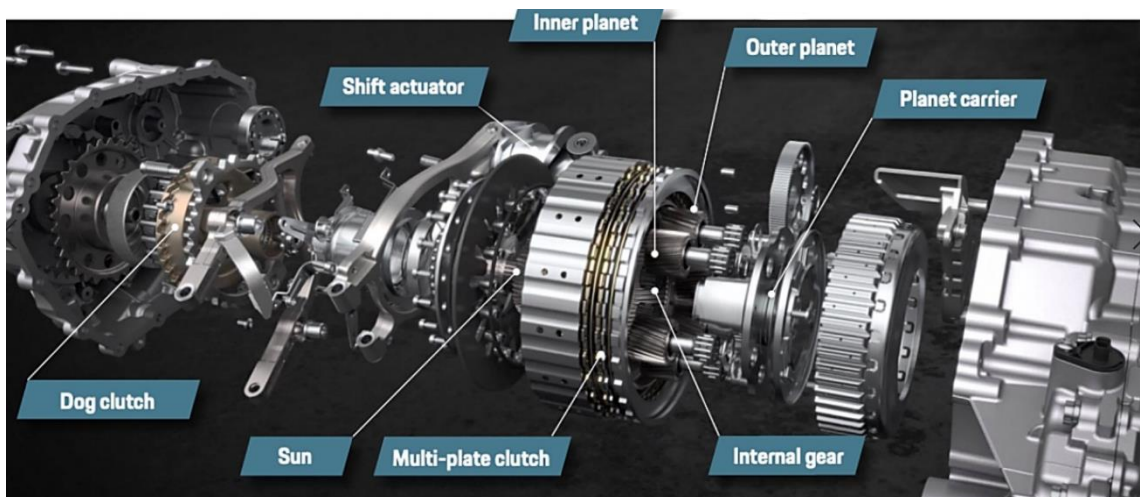


*Figure 6 - Multi speed transmission – Porsche Taycan [7]*

Figure 6 shows the actuator, which actuates two levers, connected with a dog clutch and a multi-plate clutch. Inside the multi-plate clutch there is a planetary gear set that provides the ratio for the first gear. When the first gear is engaged, the multi-plate clutch is open and the dog clutch is closed, with the planetary gear set yielding a first gear ratio. When shifting to second gear, the dog clutch opens, and the multi-plate clutch is

closed, blocking the planetary gear set, hence the gear ratio is changed and second gear is engaged. This configuration allows second gear to be shifted under full load without interruption of the torque flow. The second gear is engaged under full load at 60 km/h. [7]

## 1.3 ELECTRIC MOTORS

An electric motor is an electric machine which converts electrical energy into mechanical energy. The function is based on the interaction between electric current in a wire winding and the magnetic field (electromagnetic induction). The basic classification of electric motors is by the power source type. The motor can be powered by direct current (DC) or by alternating current (AC). Nowadays, every mass produced electric vehicle is equipped with AC motor [23].

There are several reasons why the popularity of electric motors increases. The major and the most important one is environmental friendliness connected with stricter emissions standards year after year. In contrast to the internal combustion engine, electric motor produces zero emissions such as carbon or nitrous oxides while converting electrical energy into mechanical energy. However, if we consider the production of electricity, carbon footprint depends on the type of power plant where the electric energy for charging of car batteries is produced.

One of the basic features of electric motors is their capability to produce maximal torque from almost zero RPM. In the automotive industry this capability is highly beneficial in terms of acceleration, especially while driving in the city, where a vehicle is regularly accelerating from zero speed or in the Motorsport application when a rapid increase in speed is advantageous.

Regarding the energy conversion efficiency, modern electric motors achieve average efficiency between 90-95%. The excess energy is dissipated as heat into the surroundings. When the precise determination of the efficiency for various RPM and torque is required, every motor has a specific characteristic including efficiency islands, similar to the internal combustion engines. Such characteristics can be seen in the Figure 7 [8]
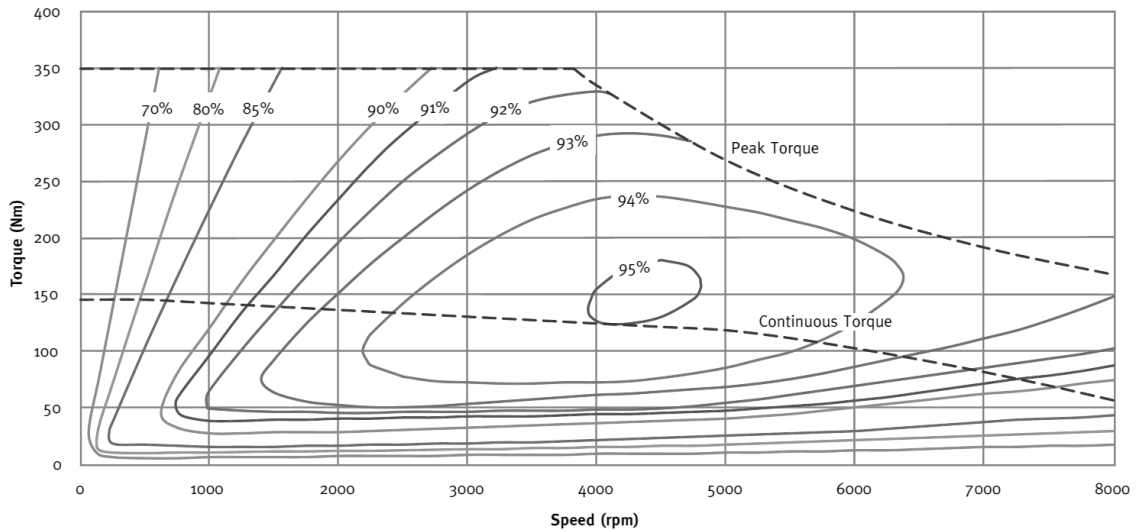
*Figure 7 – Electric motor performance and efficiency [9]*

### 1.3.1 PERMANENT MAGNET SYNCHRONOUS MOTORS

Permanent magnet synchronous motor (PMSM) is a rotating electrical machine supplied by alternating current. This type of motor consists of a 3 phase current winding that creates a magnetic field powered from the inventor (stator) and permanent magnets attached to the rotor (Figure 8). It is called synchronous because the rotor rotates at the same speed as the generated magnetic field in the stator, thus the rotation period is equal to the number of AC cycles.

The single PMSM motor can be used as a propulsion motor or as a generator. The second feature is very useful in automotive industry applications in order to generate alternating current while the vehicle is not accelerating and braking. This alternating current is then converted to direct the current via an inverter and then stored as an energy in the car´s battery pack.
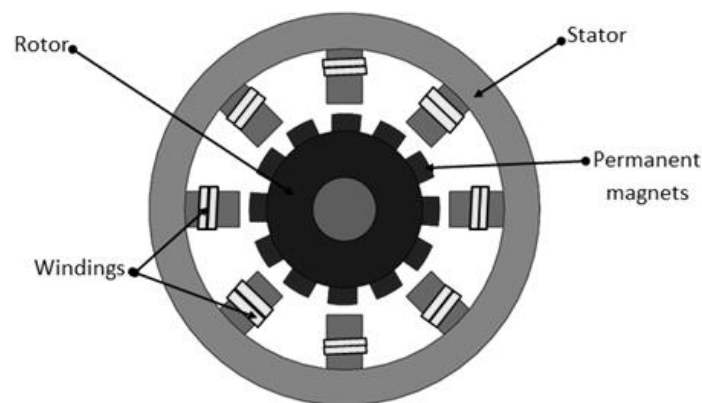


*Figure 8 - Permanent magnet synchronous motor [10]*

PMSMs are widely used in the automotive industry on account of brushless construction that improves both efficiency in a large range of RPMs and reliability. Due to the permanent magnet rotor they are able to achieve high power-to-size ratio. The absence of the slip between the magnetic field generated in the stator and the rotor's speed allows to produce torque from zero RPM.

On the other hand PMSM requires complicated control mechanism with dedicated control units that manage rotating speed. Due to that, acquisition and maintenance costs are significantly higher in contrast with AC induction motors. [11], [24]

## 1.3.2  AC INDUCTION MOTORS

An induction motor, sometimes called asynchronous motor is an electric device operating on alternating current. Electric current in the rotor, necessary to produce torque is generated by electromagnetic induction from the stator magnetic field. The name asynchronous is used, because the rotor does not rotate at the same speed as the generated magnetic field in the stator. For the induction of the rotor currents, the speed of the rotor itself must be lower than the speed of the stator rotating the magnetic field (synchronous speed). Otherwise the magnetic field would not be moving relative to the rotor conductors and no currents would be induced. The lower rotor's speed drops below synchronous speed, the more torque is created. Similarly, like the permanent magnet synchronous motor, single ACIM can be used as a propulsion motor and as a generator to recuperate energy.

The AC induction motor is the most common motor type, used in a great variety of applications. Its simple brushless design makes it highly reliable and allows it to be manufactured at a low cost.

Yet, the ACIM is less efficient (85-92%) than PMSM, which is partially related to the higher heat generation in rotor windings. Also, in order to change the speed or torque, it is necessary to undergo a relatively complex process (variable frequency drive), which is a major disadvantage in electric vehicles where frequent speed changes are a matter of course. Due to these reasons, the majority of car manufacturers prioritize permanent magnet synchronous motor in electric vehicles. Until recently, the carmaker Tesla, which equipped its models with the asynchronous induction electric motor, was one of the exceptions. However, the latest Tesla Model 3 already uses a synchronous motor with permanent magnets. [12], [24]

## 1.4 DETERMINATION OF VEHICLE PERFORMANCE

Vehicle performance is the study of the motion of a vehicle. Car performance depends on numerous variables such as engine output, transmission, driving resistance and other factors. We can determine the performance of a vehicle either experimentally (direct measurement on a dynamometer) or by software simulation of the process. [25]

### 1.4.1 MEASUREMENT ON A DYNAMOMETER

A dynamometer is a laboratory experimental tool that measures vehicle/engine output performance. Using a chassis dynamometer (driving a car on the roller), output torque at an operating speed can be directly measured. All other variables are calculated based on known design. Testing takes place in laboratory conditions, hence motion resistance such as rolling or air resistance have to be applied to the vehicle by increasing the braking force of vehicle wheels. Dynamometer test beds are usually equipped with auxiliary measuring tools to determine, for example, car emissions or fuel consumption.

The major benefit of a direct measurement is its accuracy and veridicality of results compared to the data acquired by the simulation process. Compared to simulation, the measuring process is considerably more time consuming and costly. The chassis dynamometer also has limitations in terms of maximal wheelbase, weight or top speed of a vehicle. [25]

### 1.4.2 SIMULATION SOFTWARE

Software simulation is the imitation of a real process using set of mathematical formulas and computer technology. It is experimental method, in which the real system is replaced by computer model. Experiments are performed on this model, subsequently they are evaluated, optimized and results are applied back to the real system.

The simulation makes possible to examine all aspects of the proposed change without necessity to spend resources on its real world realization. The major advantage is possibility to change time flow that enables to thoroughly examine the selected phenomenon.

#### 1.4.2.1 GT-SUITE

There are several simulation softwares currently available on the market. Among these, the GT-SUITE seems most suitable for vehicle simulations due to its user friendly interface and complete libraries of automotive parts. The description of developers is attached below:

*„GT-SUITE is the simulation tool with capabilities and libraries aimed at a wide variety of applications and industries. It offers engineers functionalities ranging from fast concept design to detailed system or sub-system/component analyses, design optimization, and root cause investigation. The software offers a unique and comprehensive solution for modelling electrified vehicles throughout all stages of the vehicle design process. Advanced data and model management features allow user to publish libraries of components for fast and efficient vehicle architecture studies. With GT-SUITE's complete transmission library and object-oriented interface, any electrified vehicle architecture can be built and tested for fuel economy and performance." [13] [https://www.gtisoft.com/gt-suite/gt-suite-overview/]*

## 1.4.3 DRIVING CYCLES

A driving cycle is a set of specific data points that represent a vehicle's velocity as a function of time. The purpose of this cycle is to simulate real world driving in laboratory conditions, usually carried out on chassis dynamometer, in order to obtain a vehicle's fuel consumption and production of emissions.

### 1.4.3.1 WLTC

The Worldwide harmonized Light vehicles Test Cycle (WLTC) is a test executed on a chassis dynamometer for the determination of mean fuel/electric consumption and emissions and pollutants from light-duty vehicles. The WLTC cycles are part of the Worldwide harmonized Light vehicles Test Procedures (WLTP), which is divided into 4 different WLTC cycles according to the maximum speed – low (56.5 km/h), medium (76.6 km/h), high (97.4 km/h), extra high (131.3 km/h). These driving phases simulate urban, suburban, rural and highway scenarios of driving. The most common type of WLTC used for passenger cars is class 3b, dedicated to vehicles with high power – to – mass ratio and top speed over 120 km/h. Detailed description is depicted in Figure 9 below. [14]
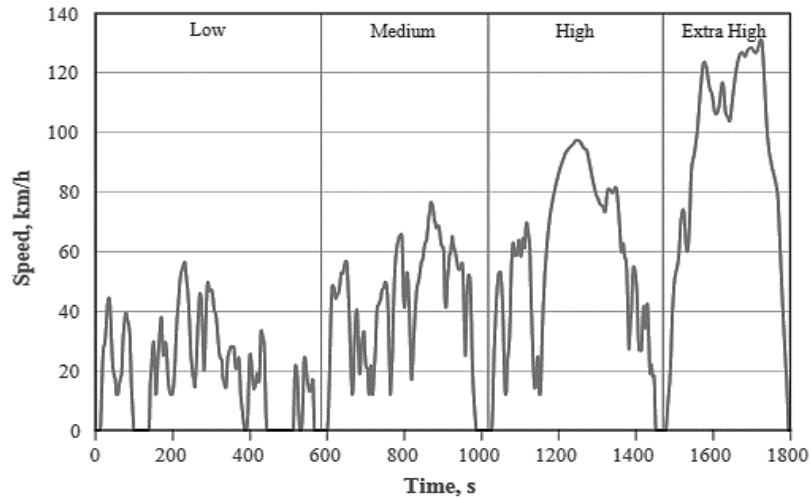
*Figure 9 - WLTC cycle for class 3b vehicles [14]*

From 1st September 2019 all the light duty vehicles that are to be registered in the EU countries must undergo and meet The Worldwide harmonized Light vehicles Test Cycle.

### 1.4.3.2  NEDC

The New European Driving Cycle is type approval testing of emissions, pollutants and fuel/electric consumption of light duty vehicles, which is performed on a chassis dynamometer. It consists of four repeated ECE-15 urban driving cycles (UDC) that represents city driving conditions such as low engine load and low speed. After 4 ECE follows the extra urban driving cycle EUDC in order to simulate more aggressive, high speed driving conditions with maximum speed of 120km/h. NEDC was firstly introduced in 1970s.

Nowadays, The New European Driving Cycle has become very outdated as driving styles have changed since the 1970's. Hence, WLTP cycle, which includes various quick accelerations and decelerations, is more accurate. [15]
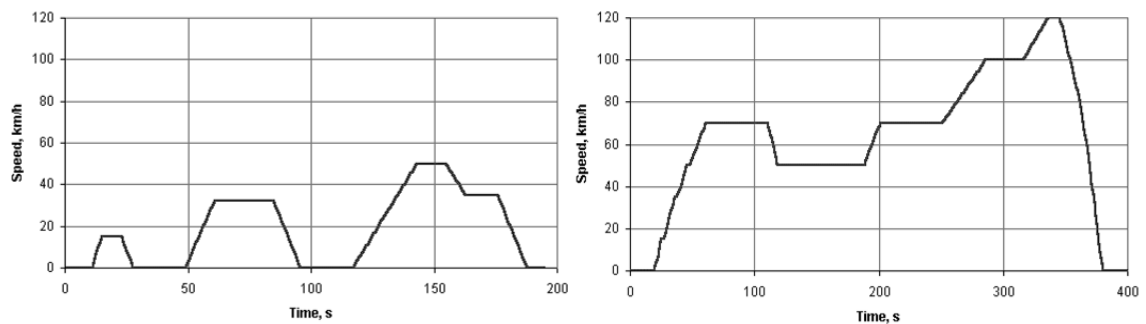


*Figure 10 - ECE-15 (left), EUDC (right) [15]*

### 1.4.3.3   EPA FEDERAL TEST PROCEDURE

The EPA federal test procedure is a series of tests introduced by the US Environmental Protection Agency in order to measure fuel economy and emissions of passenger cars. The updated procedure contains four tests: city driving (FTP-75), highway driving (HWFET) and two supplemental tests: aggressive driving (SFTP US06) and optional air conditioning test.

FTP-75 is performed on chassis dynamometer and for optimal simulation of city driving it includes 3 phases – cold start phase, stabilized phase and hot start phase.
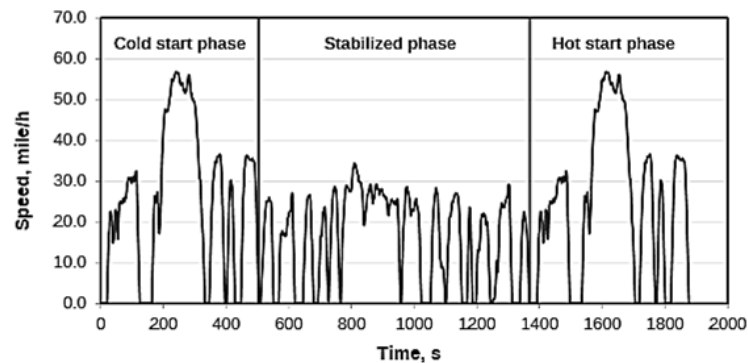


*Figure 11 - FTP-75 driving schedule [16]*

The Highway Fuel Economy Test (HWFET) cycle is a chassis dynamometer driving test which is used to determine the highway fuel economy of passenger cars. The procedure is performed twice. The first run is preparatory and the second run is the actual test with measurements. [16, 17]
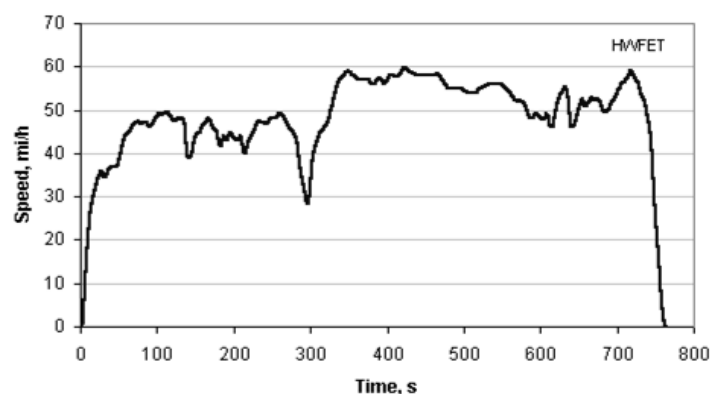


*Figure 12 - EPA Highway fuel economy test cycle [17]*

# PRACTICAL PART

The objective of this diploma thesis is to propose a layshaft gearbox for electric vehicles. The proposal will include a configuration of an electric drivetrain with a focus on the gearbox. Subsequently the vehicle parameters will be chosen for which simulation of driving on standardized driving cycle will be conducted. The aim of the simulation is to compare fixed gear, 2 and 3 speed gearbox in terms of their energy consumption. Eventually, the proposal of transmission's CAD will follow with emphasis on inner gear mechanism.

## 2.1  PERFORMANCE REQUIREMENTS

The following requirements are placed from the proposer, Ricardo s.r.o., for the propulsion system:

- Small overall dimensions
- Low weight
- Acceleration from 0 km/h to 100km/h under 7.3 seconds
- Top speed of 160km/h
- Climbing 20% slope with velocity of 80 km/h
- Electric range 250 km (WLTP measurement)
- Lifetime of 150000 km
- Gear change without interruption of power flow
- Minimal safety factor $S_F$ (bending of teeth) $S_{Fmin} = 1.05$
- Minimal safety factor $S_H$ (tooth pitting) $S_{Hmin} = 1.05$
- Minimal transverse contact ratio $\varepsilon_{min} = 3.5$

## 2.2  PARAMETERS OF THE VEHICLE

Chevrolet Bolt EV (Opel Ampera-e) (year of production 2018) was chosen as the vehicle for the procedure. The car has a front wheel drive and the powertrain is transversally mounted.  Instead of Chevrolet's original electric motor, battery pack and gearbox, the vehicle is equipped with components discussed in the following chapters in order to compare performance and energy consumption. Other technical specifications are listed below in Table 1.

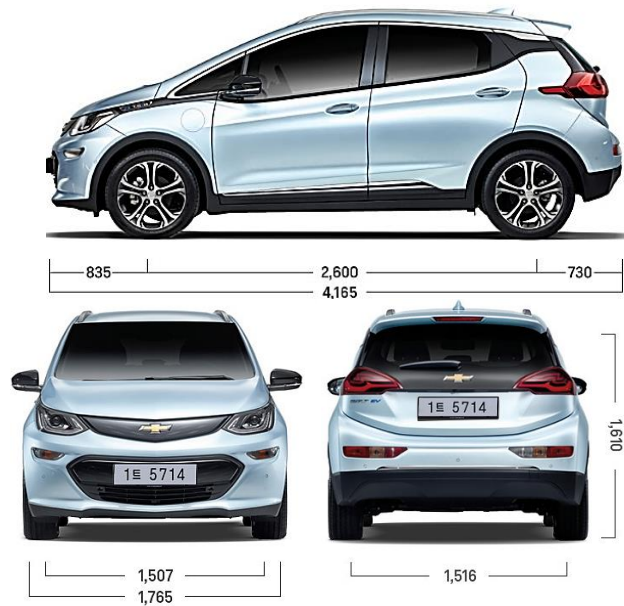| Curb Weight [kg] | 1616 |
|---|---|
| Drag Coefficient | 0.3 |
| Frontal Area [m²] | 2.22 |
| Tyre rolling resistance | 0.01 |
| Dynamic tyre diameter [m] (225/50R16) | 0.632 |
| Tyre friction coefficient | 1.1 |

*Table 1 - Chevrolet Bolt EV technical specifications [19]*



*Figure 13 - Chevrolet Bolt EV [19]*

## 2.3 POWERTRAIN CONFIGURATION

Various types of powertrain configuration of electric vehicle were mentioned in chapter 1.1. The layout where the electric motor with the gearbox are mounted transversely in the front, as can be seen in the Figure 14, is chosen for the following procedure. The clutch (dual clutch mechanism) is present in vehicles with a multi speed gearbox only. The front axle of the vehicle is powered (FWD).
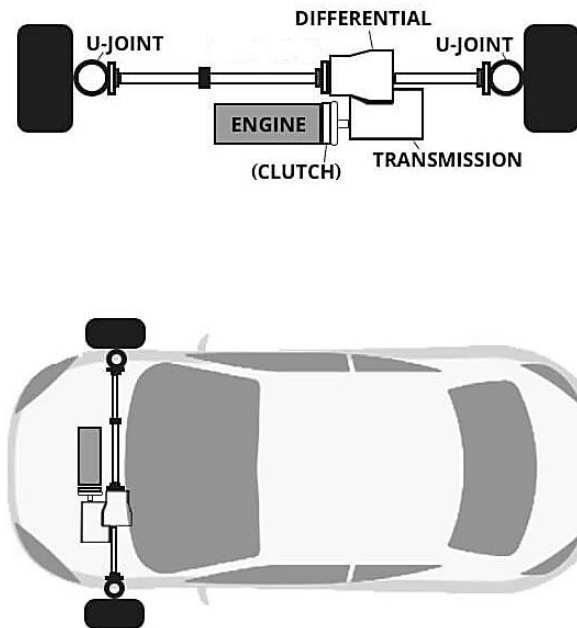




*Figure 14 - Powertrain configuration [18]*

24

The electric motor (engine) is connected via clutch to the input shaft of the gearbox. The pinion of the differential is located on the output shaft of the gearbox. The gearbox together with the differential are located in the single casing as one unit. This layout allows us to utilize fixed gear as well as multi speed gearboxes. Chosen configuration results in a space efficient packaging of whole drivetrain. Fewer powertrain parts such as shafts and clutches are needed, meaning it is lighter and cost-saving.

## 2.4  POWER REQUIREMENTS

### 2.4.1  MOTION RESISTANCE

In order to meet proposer requirements in terms of acceleration, slope driving and top speed, we have to anticipate driving resistance of the vehicle, which is made up of

- Rolling resistance $F_R$
- Air resistance $F_L$
- Gradient resistance $F_{ST}$
- Acceleration resistance $F_a$

#### 2.4.1.1  ROLLING RESISTANCE

Rolling resistance is the resistance that acts on a body of circular cross-section during its rolling movement on the surface (contact of a tyre with a road). Figure 15 shows force distribution action on a wheel during movement. Pressure distribution is asymmetrical, hence reaction R is located in front of the wheel axis by the amount of eccentricity e. [20]
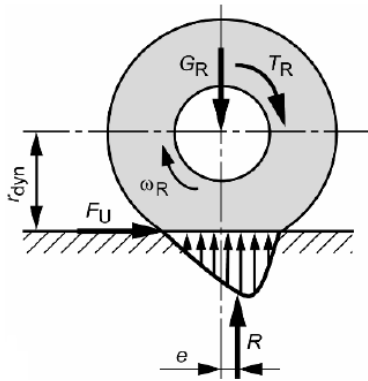


*Figure 15 - The rolling resistance [20]*

Moment equation is, then

$$-F_U = F_R = \frac{e}{r_{dyn}} \cdot R \cdot \cos(\alpha) = f_r \cdot G_R = f_r \cdot m \cdot g \cdot \cos(\alpha) \tag{1}$$

$G_R$ – wheel load [N]

$T_R$ - drive/braking torque, equal to 0 ($T_R = 0$)

$r_{dyn}$ - dynamic wheel diameter [m]

$f_r$ - rolling resistance coefficient [-]

$-F_U$ - circumferential force [N]

$g$ – Gravitational acceleration [m/s$^2$]

$m$ – mass of the vehicle [kg]

$\alpha$ – road gradient [°]

Considering the vehicle is moving on the asphalt surface, the rolling resistance coefficient $f_r = 0.01$, then

$$F_R = f_r \cdot m \cdot g \cdot cos(\alpha) = 0.01 \cdot 1616 \cdot 9.81 = 158.53 \ N \qquad (2)$$

The traction limit of the one wheel due to the tire adhesion is calculated by:

$$F_{Tlim} = m \cdot g \cdot 1.1 \cdot 0.25 = 1616 \cdot 9.81 \cdot 1.1 \cdot 0.25 = 4359 \ N \qquad (3)$$

### 2.4.1.2 AIR RESISTANCE

The air resistance acts on a body moving in gas or liquid. It always points against the direction of movement of the body. The air resistance is made up of internal resistance, surface resistance and pressure drag. Drag is calculated by [20]

$$F_L = \frac{\rho}{2} \cdot c_w \cdot A_f \cdot v^2 \qquad (4)$$

$\rho$ – air density [kg/m$^3$]

$c_w$ – drag coefficient [-]

$A_f$ – frontal area [m$^2$]

$v$ – actual vehicle speed [m/s]

### 2.4.1.3 GRADIENT RESISTANCE

Gradient resistance acts on a vehicle when it is moving on inclined or declined surface. Resistance is the result of gravitational forces. It is calculated from weight acting at the centre of gravity. [20]

$$F_{ST} = m \cdot g \cdot \sin(\alpha) \qquad (5)$$

$$\sin(\alpha) \approx \tan(\alpha) = \frac{q}{100} \qquad (6)$$

$q$ – road gradient [%]

### 2.4.1.4 ACCELERATION RESISTANCE

The final vehicle resistance is acceleration resistance, which occurs when the velocity of the vehicle is not a constant. The resistance to acceleration is influenced by two components: total mass of the vehicle and inertial mass of rotating parts during acceleration. The acceleration resistance is represented in a simplified form as [20]

$$F_a = m \cdot a \cdot \lambda \qquad (7)$$

$\lambda$ – rotation inertia coefficient, for 1$^{st}$ gear 1.3; for second gear 1.2; for 3rd gear 1.1 [-]

### 2.4.1.5 TOTAL DRIVING RESISTANCE

The traction force $F_T$ is equal to sum of all driving resistances described above and is defined as

$$F_T = f_r \cdot m \cdot g + \frac{\rho}{2} \cdot c_w \cdot A_f \cdot v^2 + m \cdot g \cdot \sin(\alpha) + m \cdot a \cdot \lambda \qquad (8)$$

For each of the three driving conditions (acceleration, top speed, slope driving), different tractive force to overcome driving resistances will be necessary.

For the acceleration from 0 km/h to 100 km/h in 7.3 seconds

$$a = \frac{\Delta v}{\Delta t} = \frac{100/3.6}{7.3} = 3.805 \; m/s^2 \qquad (9)$$

$$F_T = 0.01 \cdot 1616 \cdot 9.81 + \frac{1.225}{2} \cdot 0.3 \cdot 2.22 \cdot 13.9^2 + 0 + 1616 \cdot 3.8 \cdot 1.2$$

$$= 7616 \; N \qquad (10)$$

For climbing the slope with gradient of 20 % at a speed of 80 km/h

$$F_T = 0.01 \cdot 1616 \cdot 9.81 \cdot \cos(0.2) + \frac{1.225}{2} \cdot 0.3 \cdot 2.22 \cdot 22.2^2 + 1616 \cdot 9.81 \cdot \sin(0.2)$$

$$= 3465.9 \; N \qquad (11)$$

For driving at a speed of 160 km/h

$$F_T = 0.01 \cdot 1616 \cdot 9.81 + \frac{1.225}{2} \cdot 0.3 \cdot 2.22 \cdot 44.44^2 + 0 + 0 = 964.3N \quad (12)$$

## 2.4.2 MINUMUM ENGINE POWER

After obtaining tractive force to overcome motion resistance, required engine power can be calculated using formula (13). The results for each of the three driving conditions are stated in Table 2 below.

$$P_e = F_T \cdot v \cdot \eta \qquad (13)$$

$\eta$ – efficiency of the drivetrain, assumed to be 0.9 [-]

| | Electric motor power $P_e$ [kW] |
|---|---|
| **Acceleration** | 117.53 |
| **Uphill ride** | 85.58 |
| **Top speed** | 47.62 |

*Table 2 – Minimum required power of electric motor*

According to the Table 2 above we can summarize that an electric motor with minimal power output of 118 kW is necessary to fulfil driving conditions.

## 2.5  TRACTION MOTOR

For the propulsion of the vehicle a three phase synchronous motor with permanent magnets is used due to its popularity among car manufacturers. In order to take advantage of the various types of transmissions, every gearbox type is paired with a different electric motor. The specifications of each motor were chosen in order to fulfil the vehicle's performance requirements given by the proposer, with respect to the calculations done in chapter 2.4.1. To avoid deviations caused by theoretical computations of driving resistances, electric motors with slightly higher power outputs were used for the following simulation purposes.

By equipping a vehicle with a multi – gear gearbox less powerful traction motor can be used, compared to fixed gear transmission, in order to meet performance requirements as it was stated in chapters 1.2 and 1.3. Less powerful motor has smaller dimensions and weight that create significant advantage in automotive applications. In the Table 3 below, basic performance parameters of all three motors are listed. Motor performance characteristics for both peak and continuous output of 120kw engine can be seen in Figure 16.

| | Fixed gear gearbox | Two speed gearbox | Three speed gearbox |
|---|---|---|---|
| **Max Peak Power [kW]** | 130 | 120 | 115 |
| **Max Continuous Power [kW]** | 63 | 58 | 56 |
| **Max Peak Torque [Nm]** | 272 | 252 | 241 |
| **Max Continuous Torque [Nm]** | 113 | 105 | 100 |
| **Max peak output duration [s]** | 30 | 30 | 30 |
| **Maximal RPM [min$^{-1}$]** | 12000 | 12000 | 12000 |
| **Efficiency [%]** | 80-95% | 80-95% | 80-95% |
| **Weight [kg]** | 57.5 | 47.5 | 42.5 |
| **Max supply voltage [VDC]** | 720 | 720 | 720 |

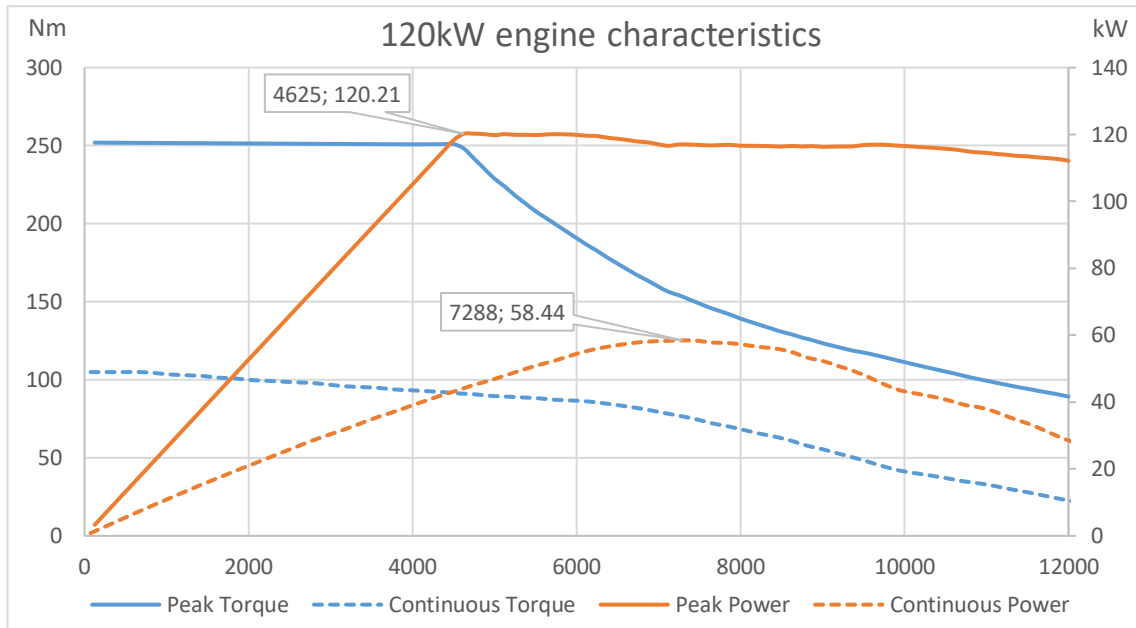*Table 3 - Permanent magnet synchronous motors characteristics*

*Figure 16 - Engine performance characteristics*

## 2.6  TRANSMISSION

### 2.6.1  GEARBOX LAYOUT

Electric vehicle transmissions were described in detail in chapter 1.2.2. One of the proposer's requirements was to design a layshaft transmission with helical gears. Based on this requirement, 3 types of gearboxes were used for the following comparison. The first one is fixed gear, parallel layshaft transmission (Figure 18), with constant gear and final drive ratio. The second model is a two speed dual-clutch transmission with two synchronizers (Figure 17) that allow to change gears without interruption of the power flow. During the acceleration from standstill, the first gear is engaged. A sensor detects the engine's RPM. Once the engine meets critical revs, the second gear is engaged via a clutch and synchronizer mechanism. The last one is a three speed dual-clutch transmission with three synchronizers (Figure 19) which works on the same principle as the previous gearbox.
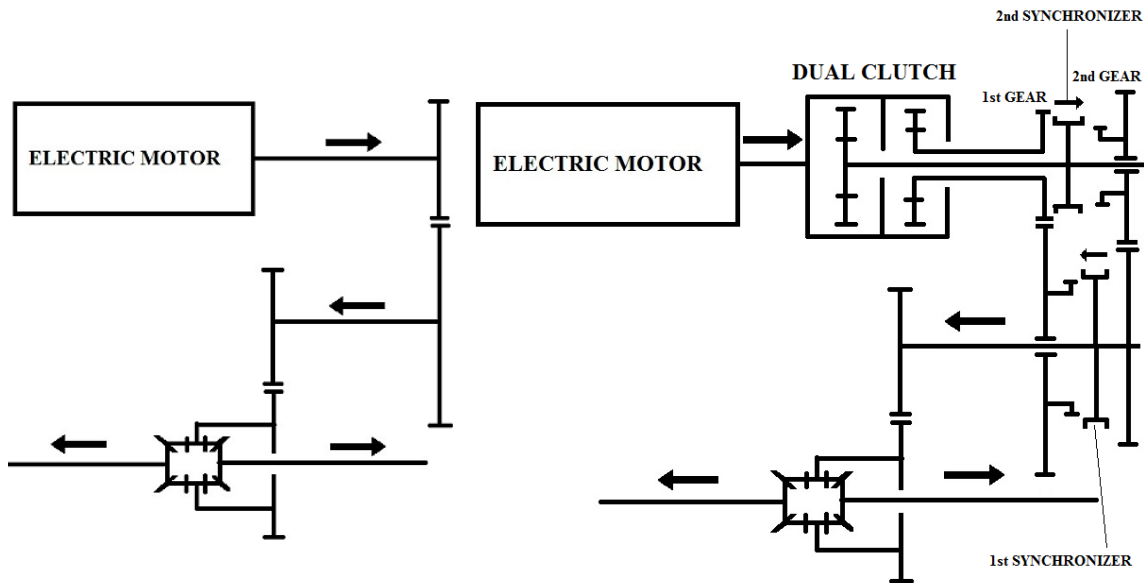
*Figure 18 - Fixed gear parallel layshaft transmission*

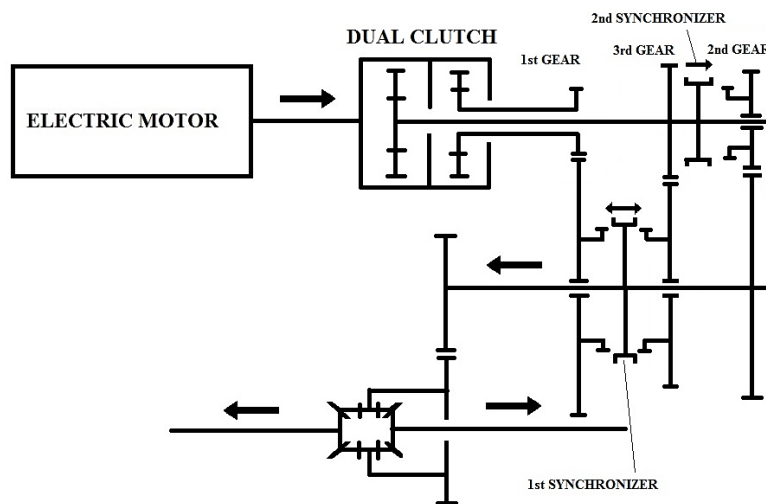*Figure 17 - Two speed dual-clutch transmission*



*Figure 19 - Three speed dual-clutch transmission*

## 2.6.2 PRELIMINARY GEAR RATIOS

In passenger vehicles, the output conversion between the driven wheels and the engine is obtained by the combined action of the powertrain assemblies. Total gear ratio $i_t$ – ratio between output and input speed, of the powertrain is achieved from the ratio of the transmission $i_G$ and the ratio of final drive $i_F$. The ratios have to be designed to enable vehicle to:

- Reach required maximum speed
- Operate in efficient range of engine's RPM
- Accelerate within required time [20]

For the simulation purposes, it is not necessary to divide gear ratio between final drive and gearbox, hence only total gear ratio of each of the three powertrains will be designed.

To propose gear ratio for the single speed fixed gear gearbox, the biggest limitation is the electric motor's maximum RPM (12000 min-1). In order to meet both acceleration and top speed requirements, the biggest ratio that enables the vehicle to reach 160 km/h (44.4 m/s) should be used. In this case

$$n_w = \frac{v}{\pi \cdot d_{tyre}} \cdot 60 = \frac{44.44}{\pi \cdot 0.632} \cdot 60 = 1342 \ min^{-1} \tag{14}$$

$$i'_{t1} = \frac{n_{Emax}}{n_w} = \frac{12000}{1342} = 8.94 \tag{15}$$

$\eta_w$ – wheel RPM at 160km/h [min$^{-1}$]

$d_{tyre}$ – dynamic diameter of tyre [m]

$i'_{t1}$ – total preliminary gear ratio of single speed powertrain

$\eta_{Emax}$ – maximum engine RPM [min$^{-1}$]

A different procedure has to follow for the remaining multi speed gearboxes, where the first gear provides the vehicle's acceleration and the other gears should be proposed to enable the electric motor to operate in the efficient range of RPM. In addition, a fixed RPM for upshifts and downshifts should be set for each gear.

Multi speed dual clutch transmissions are paired with less powerful engines. Thus first gear ratio has to be higher than 8.94 to meet acceleration requirements. The second/third gear ratio was proposed so that the engine will operate at the highest possible efficiency during a highway ride at 130km/h. Engagement of the higher gear occurs when the engine starts operating at a high RPM, hence the efficiency is lower. A downshift happens, when RPM of the engine decreases below the critical value where the efficiency is not satisfactory.

The proposal of preliminary gear ratios for both multispeed gearboxes includes an iteration process performed in the simulation software to achieve appropriate values that meet the conditions discussed in the beginning of this chapter. Results for each gearbox are listed in Table 4 below.

| | Fixed gear gearbox | Two speed gearbox | Three speed gearbox |
|---|---|---|---|
| Total gear ratio for 1st gear $i'_{t1}$ | **8.94** | **12.02** | **14.51** |
| RPM for upshift to 2nd gear     [min⁻¹] | - | 7750 (77 km/h) | 6500 (53 km/h) |
| Total gear ratio for 2nd gear $i'_{t2}$ | - | **5.8** | **8.1** |
| RPM for downshift to 1st gear  [min⁻¹] | - | 3000 | 3700 |
| RPM for upshift to 3rd gear     [min⁻¹] | - | - | 6800 (101 km/h) |
| Total gear ratio for 3rd gear $i'_{t3}$ | - | - | **5.49** |
| RPM for downshift to 2nd gear [min⁻¹] | - | - | 4300 |

*Table 4 - Gear ratios and critical motor RPM for gear changes*

## 2.7  BATTERY PACK

The energy for the traction motor is stored in lithium-ion batteries, which are suitable for repetitive charging and discharging. That is why this type of batteries is commonly used to power electric vehicles. Battery pack specifications are listed below in Table 5.

| Battery type | Li-ion |
|---|---|
| Nominal voltage [V] | 3.7 |
| Cell capacity [Ah] | 37 |
| Number of series cells | 104 |
| Number of parallel cells | 4 |
| Total capacity of the storage system [kWh] | 56.95 |
| Useful capacity of the storage system [kWh] | 48.41 |
| Maximum charge voltage limit [V] | 385 |
| Maximum discharge voltage limit [V] | 330 |
| Total weight of the battery pack [kg] | 400 |

*Table 5 – Battery pack specifications*

## 2.8  SIMULATION OF DRIVING

According to the chapter 1.4, I decided to perform a software simulation of the driving to acquire vehicle performance. GT – suite 2019 was used as the simulation software. Three virtual vehicles with the same parameters, listed in the Table 1 except of traction motors and gearboxes (discussed in chapters 2.5 and 2.6) were used to simulate the real world driving. The model of the vehicle is shown in the Figure 20.
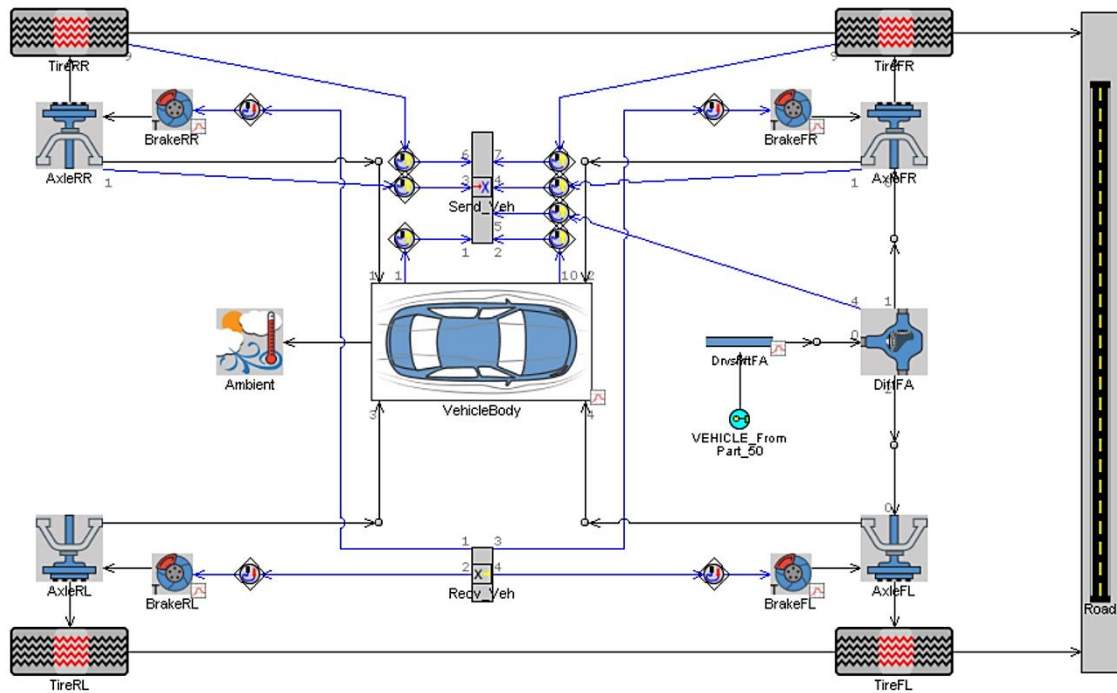


*Figure 20 – GT – Suite model of the vehicle*

The aim of the simulation was to investigate if every vehicle is able to meet the performance requirements – acceleration from 0 km/h to 100 km/h in 7.3 seconds, top speed of 150 km/h, climbing 20 % slope with velocity of 80 km/h and WLTP range of 250 km.

In the second part of the simulation process, the focus was on electric consumption during driving according to the WLTP driving cycle and highway cruising at 130 km/h, comparison of all three vehicles, and an evaluation of the results.

### 2.8.1  ACCELERATION

The software simulates the acceleration of vehicles from standstill to 100 km/h, taking into account motion resistance. As can be seen in Table 6, all three vehicles meet the acceleration requirements. Results indicate that vehicles equipped with the multi speed gearboxes, even if they are powered by the less powerful motors, are able to

accelerate faster than the single speed one. It is caused by the higher first gear ratio of the multi speed gearboxes, which multiplies motor torque thus increasing the tractive force of the wheels.

| | Fixed gear gearbox | Two speed gearbox | Three speed gearbox |
|---|---|---|---|
| 0 – 100 km/h [s] | 7.3 | 7.26 | 7.16 |

*Table 6 – Acceleration from 0 km/h to 100 km/h*

### 2.8.2 UPHILL RIDE

The software simulation of a vehicle driving uphill on the slope of 20 % with the constant velocity of 80 km/h confirms the results obtained in Chapter 2.4.2. The minimum power required for this kind of drive is approximately 77 kW. Due to the efficiency of the drivetrain that assumed to be 0.9, the minimal engine power is 85 kW. Every vehicle is equipped with the more powerful motor than 85 kW; therefore, it meets the requirement.

According to the results, different types of gearbox do not provide any advantage in this particular discipline. The only difference is in the energy consumption, which is directly connected to motor efficiency. A three speed gearbox enables the motor to operate in more efficient range than the other two gearboxes. However, the difference in energy consumption was negligible, so this phenomenon was not further investigated.

### 2.8.3 TOP SPEED

The top speed of every vehicle was obtained by the simulation of wide open throttle acceleration from the standstill, until the point when the vehicle is not further accelerating or the electric motor reaches maximal operating RPM. In this type of driving, when high power output for a long period of time is required, we have to take into account the motor's maximum peak output duration which is 30 s for each motor. After that period, the motor ECU limits power output to continuous values. Figure 21 shows the top speed of all three vehicles equipped with different types of gearboxes.

In the first case (red line), the limitation for the top speed is the maximal RPM of the electric motor, that is 12000 min$^{-1}$. The gear ratio of the fixed gear gearbox was selected with respect to the required top speed – 160 km/h. The vehicle is able to reach

160 km/h and further acceleration is electronically restricted by the ECU of the electric motor.

The blue line shows the top speed of the vehicle equipped with a 2 speed gearbox. In this case, the maximum value is limited by the peak output duration time (30 s). During this period of time, the vehicle accelerates up to 191 km/h. The power is then lowered to the continuous value and the vehicle is not able to overcome driving resistances so it starts to slow down. To prevent this from happening, top speed is electronically limited to 180 km/h – velocity at which the vehicle can travel using continuous output characteristics of the 120 kW electric motor.

The green line shows the top speed of the vehicle equipped with a three speed gearbox. The results are similar to the previous case. The same problem with peak duration time occurs, so the theoretical top speed is 189 km/h, but it has to be lowered. The top speed is limited to 178 km/h, respecting the 115 kW motor continuous output characteristics.
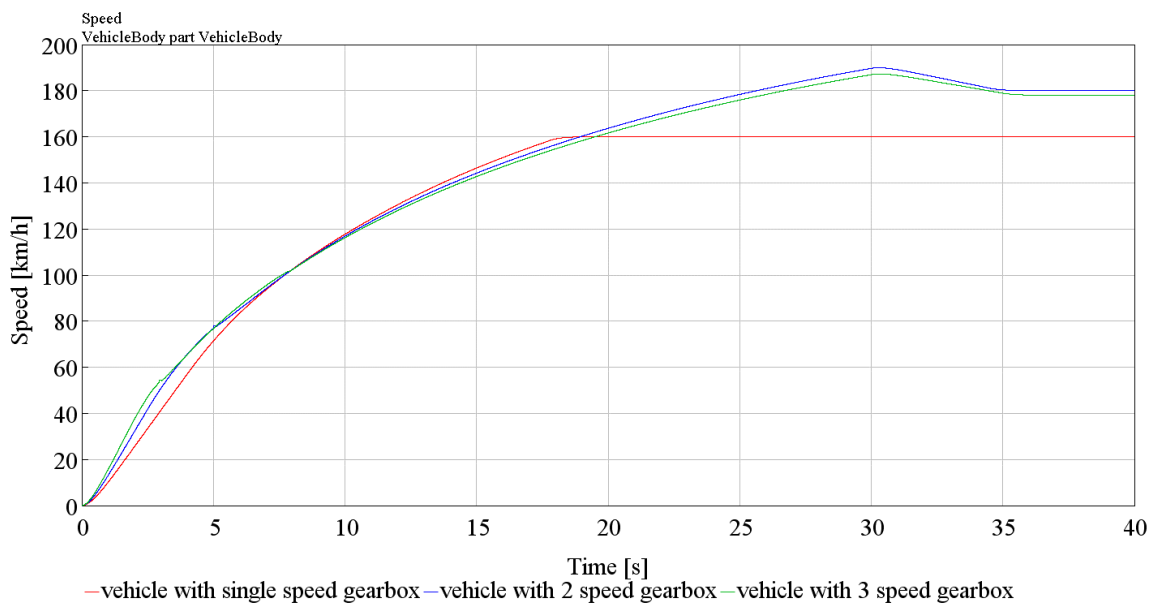


*Figure 21 – Top speed*

## 2.8.4   SIMULATION OF HIGHWAY DRIVING

The simulation of the highway driving consists of 217 km course, where vehicle cruise at 130 km/h, which will take 100 minutes. Preliminary second and third gear ratios were designed in order to enable motor work in the most efficient range of RPM especially during high speed rides.

The consumption of electrical energy during the highway test course for every vehicle is listed below in the Table 7.

35

|  | Fixed gear gearbox | Two speed gearbox | Three speed gearbox |
|---|---|---|---|
| **Energy consumption [kWh/100km]** | 20.63 | 19.85 | 19.81 |
| **Total energy consumption [kWh]** | 48.02 | 46.26 | 46.16 |
| **Initial state of charge (SOC) [%]** | 95 | 95 | 95 |
| **Final SOC [%]** | 10.68 | 13.77 | 13.93 |

*Table 7 – Energy consumption during the highway test course*
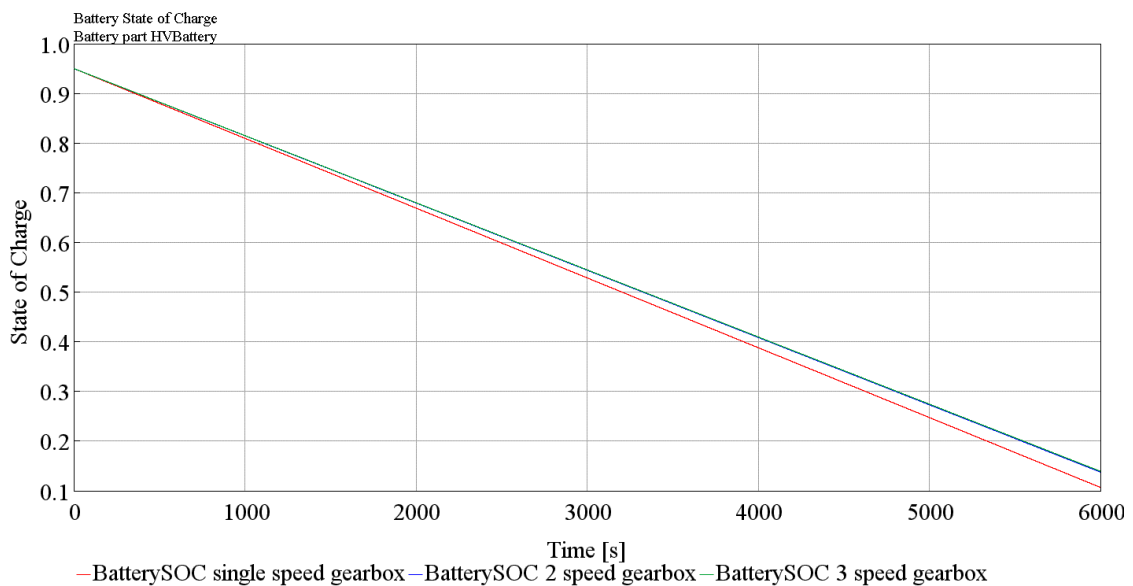


*Figure 22 – Battery SOC during highway test*

According to the energy consumption data, the most efficient is the vehicle equipped with the three speed gearbox. Total $3^{rd}$ gear ratio of 5.49 allows the motor to operate with the efficiency of 94.1 %. For the comparison, the motor paired with fixed gear gearbox (total gear ratio 8.9) reach efficiency of 90.5 % during highway cruising.

Results indicated that the difference between the two and three speed gearbox in terms of battery energy consumptions is only 0.04 kWh/100 km. From this point of view, the advantage of the three speed gearbox is negligible.

## 2.8.5 SIMULATION OF THE STANDARDIZED DRIVING CYCLE

Among driving cycles discussed in the chapter 1.4.3, WLTP driving cycle was chosen for the purposes of the simulation due to the fact that from 1st September 2019 all

the light duty vehicles that are to be registered in the EU countries must undergo and meet The Worldwide harmonized Light vehicles Test Cycle.

The procedure consists of 15 consecutive WLTC with the total distance traveled of 348.9 km and the overall simulation duration of 7.5 hours. Each car meet the minimal required electric range of 250 km. Vehicles start with the battery state of charge (SOC) of 95 %. After the completion of the test, vehicles SOC should not fall below 10 %. Usable battery capacity was limited to 95-10 %, to enhance battery lifetime.

Detailed results of the test procedure are listed below in Table 8.

|  | Fixed gear gearbox | Two speed gearbox | Three speed gearbox |
|---|---|---|---|
| **Energy consumption [kWh/100km]** | 12.02 | 11.86 | 11.80 |
| **Total energy consumption [kWh]** | 45.34 | 44.59 | 44.35 |
| **Average motor efficiency [%]** | 71.1 | 71.2 | 71.6 |
| **Average motor power losses [kW]** | 0.84 | 0.73 | 0.71 |
| **Initial state of charge (SOC) [%]** | 95 | 95 | 95 |
| **Final SOC [%]** | 15.39 | 16.71 | 17.13 |

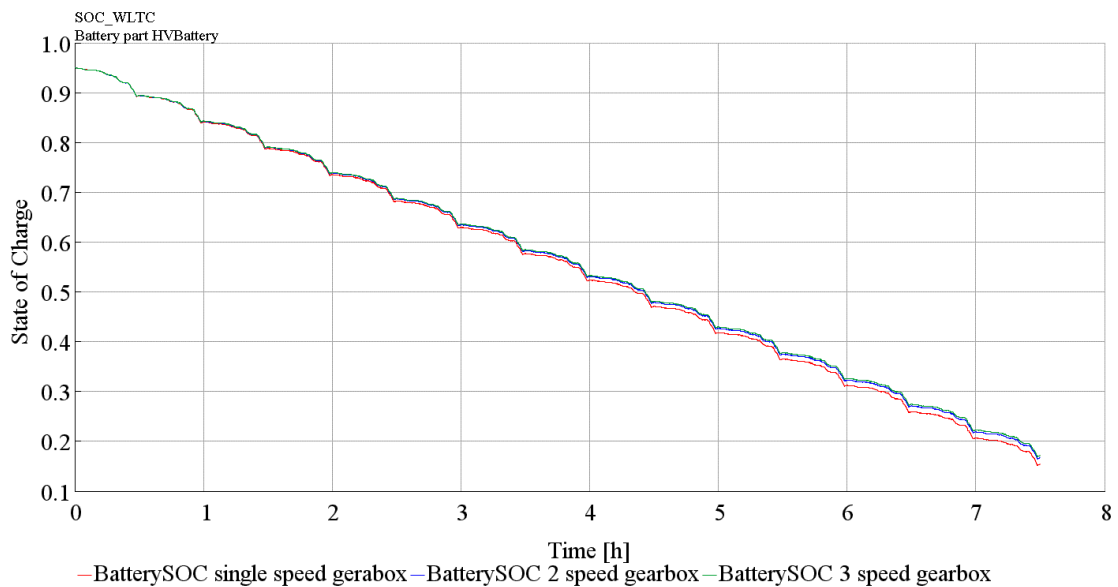*Table 8 – Energy consumption during 15 consecutive WLTC*



*Figure 23 – Battery SOC during 15 consecutive WLTC*

Results indicate that vehicle equipped with the three speed gearbox achieves the highest motor efficiency, thus the energy consumption is the lowest among all three vehicles.

## 2.8.6 EVALUATION OF THE RESULTS

The simulation of various driving courses enables a direct comparison of singe, two and three speed gearbox paired with the 130, 120 and 115 kW electric motors. Every vehicle fulfills performance requirements stated in Chapter 2.1. Acceleration data confirm that by the equipping vehicle with the multi speed transmission, a less powerful motor can be utilized to achieve similar performance than the single speed gearbox vehicle.

The advantage of the second/third gear with a lower gear ratio is that the vehicle can reach a higher top speed – 180 km/h instead of 160 km/h, because it is not limited by the motor maximal RPM but by the motor's continuous power output.

According to the highway drive average energy consumption, the difference between single and two speed gearbox while traveling with the velocity of 130 km/h is 0.78 kWh/100km. The second gear reduces average electric energy consumption by 3.8 % on the highway. The difference in the average consumption, between two and three speed gearbox is only 0.04 kWh/100km. We can see that third gear provides only an insignificant advantage compared to the second gear in terms of electrical energy consumption.

The most important measurement was the Worldwide harmonized Light vehicles Test Cycle. During this cycle, the energy consumption, efficiency of the motor and battery SOC were observed. The results indicate that the highest efficiency, thus the lowest average energy consumption, is achieved by an electric motor paired with the three speed transmission. Throughout WLTC the second gear reduces average energy consumption per 100 kilometers by 1.34 % and the vehicle equipped with the three speed gearbox reduces consumption by 1.83 %.

Having reviewed the energy consumption data, we can summarize that adding one more gear to the fixed gear gearbox reduces average consumption up to 3.8 % on the highway. On the other hand, the use of three speed gearbox reduces consumption by only 0.5 - 0.8 % compared to the 2 speed gearbox.

As was stated in Chapter 1.2.2, thanks to the multi speed gearbox the vehicle can be powered by the electric motor with a lower power output then the motor in the single speed one. The less powerful motor is lighter, smaller and less expensive. According to

Table 3, the weight difference between 130 kW and 120 kW engines is 10 kg. In contrast with that, we can assume that the weight of the multi speed gearbox is higher, due to the necessity to use a second gear pair, dual clutch and synchronizer mechanisms. By taking into account the energy consumption, weight and acquisition costs, the two speed dual clutch gearbox is the most suitable gearbox for the chosen vehicle.

## 2.9 PROPOSAL OF THE GEARBOX

### 2.9.1 GEARBOX CONFIGURATION

After taking into account the results obtained from the simulation of the driving, the vehicle described in Chapter 2.2 will be equipped with the two speed dual clutch gearbox that will power the front axle. The gearbox configuration is shown in Figure 24 below.
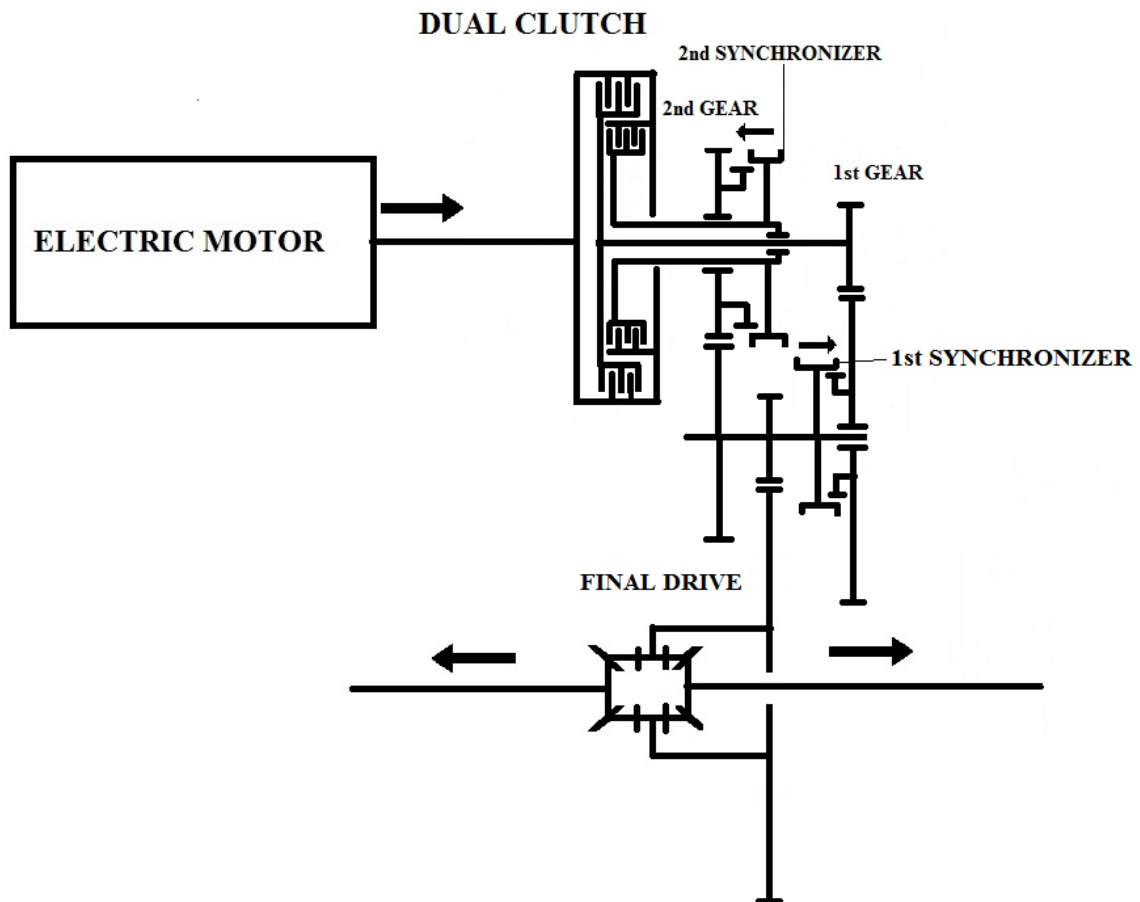


*Figure 24 – Dual clutch 2 speed gearbox*

## 2.9.2 GEAR RATIOS

During the proposal of gearbox gear ratio, the total preliminary powertrain ratio for both the first and the second gear stated in the 2.6.2 has to be adhered and divided between the gearbox ratio $i_g$ and the final drive ratio $i_f$ respecting the formula below.

$$i_t = i_g \cdot i_f \tag{16}$$

The vehicle is equipped with the final drive, which yields gear ratio of $i_f = 4.117$. The actual gearbox ratio along with the number of teeth, listed in the Table 9, for the pinion ($z_1$) and wheel ($z_2$) can be calculated using the equation 16 and 17.

$$i_g = \frac{z_2}{z_1} \tag{17}$$

|  | 1st gear | | 2nd gear | | Final drive | |
|---|---|---|---|---|---|---|
|  | Pinion | Wheel | Pinion | Wheel | Pinion | Wheel |
| **Number of teeth z** | $z_1 = 22$ | $z_2 = 64$ | $z_3 = 32$ | $z_4 = 45$ | $z_{f1} = 17$ | $z_{f2} = 70$ |
| **Actual gear ratio i** | $i_{g1} = 2.909$ | | $i_{g2} = 1.406$ | | $i_f = 4.117$ | |
| **Total gear ratio $i_t$** | $i_{t1} = 11.979$ | | $i_{t2} = 5.79$ | | - | |

*Table 9 – Gear ratio and number of teeth of every gear pair*

## 2.9.3 GEAR GEOMETRY

The gearbox is fitted with two pairs of helical gears that yield 2 gears. Located on the output shaft (counter shaft) is a final drive pinion paired with the final drive wheel on the differential assembly. A necessary condition during the proposal process was to choose the axial (center) distance which has to be the same for both the first speed and the second speed.

### 2.9.3.1 INPUT PARAMETERS

The calculation of the gear geometry was based on the input parameters, listed in Table 10. First, during the iteration process, the modulus and the helix angle for both gear pairs were chosen so that the axial distance was the same for both gear pairs. Subsequently, the face width of gears was proposed in order to meet safety factors and total contact ratio.

| | 1st speed | | 2nd speed | | Final drive | |
|---|---|---|---|---|---|---|
| | Pinion | Wheel | Pinion | Wheel | Pinion | Wheel |
| **Normal modulus $m_n$ [mm]** | 1.6 | | 1.8 | | 2.5 | |
| **Helix angle $ß$ [°]** | 30 | | 30 | | 30 | |
| **Face width $b$ [mm]** | 24.5 | 23.1 | 26.5 | 25.4 | 37 | 35.3 |
| **Normal pressure angle $\alpha_n$ [°]** | 20 | | 20 | | 20 | |
| **Addendum clearance $c_a$** | 0.25 | | 0.25 | | 0.25 | |
| **Relative addendum $h^*_a$** | 1 | | 1 | | 1 | |

*Table 10 – Input parameters*

### 2.9.3.2 AXIAL DISTANCES AND CORRECTIONS DISTRIBUTION

Preliminary axial distance $a$ is calculated using formula (18). Rounding the value we obtain the actual axial distance $a_w$ between each input shaft and gearbox output shaft (countershaft).

$$a = \frac{m_n}{2 \cdot cos(\beta)} \cdot (z_1 + z_2) \tag{18}$$

Due to the differences between calculated and actual axis distances, the total profile shift coefficient $x$ is introduced. It is divided between the pinion and the wheel in order to prevent undercutting of teeth. The total profile shift coefficient and its distribution are calculated using the equations (19) - (23). The results are stated in the Table 11.

$$\alpha_t = arctg \frac{tg\,\alpha_n}{cos ß} \tag{19}$$

$$\alpha_W = arcos \left( \frac{a}{a_w} \cdot cos\alpha_t \right) \tag{20}$$

$$inv\,\alpha_t = tg\,\alpha_t - \alpha_t \cdot \frac{\pi}{180} \tag{21}$$

$$inv\,\alpha_W = tg\,\alpha_W - \alpha_W \cdot \frac{\pi}{180} \tag{22}$$

$$x_1 + x_2 = \frac{z_1 + z_2}{2 \cdot tg(\alpha_n)} \cdot (inv\,\alpha_W - inv\,\alpha_t) \tag{23}$$

|  | 1st speed | 2nd speed | Final drive |
|---|---|---|---|
| Preliminary axial distance $a_w$ [mm] | 79.45 | 80.02 | 125.57 |
| Actual axial distance $a$ [mm] | 80 | 80 | 125 |
| Transverse pressure angle $\alpha_t$ [°] | 22.8 | 22.8 | 22.8 |
| Rolling pressure angle $\alpha_W$ [°] | 23.7 | 22.7 | 22.2 |
| Transverse involute $inv\ \alpha_t$ [-] | 0.02241 | 0.02241 | 0.02241 |
| Rolling involute $inv\ \alpha_W$ [-] | 0.0254 | 0.0223 | 0.02052 |
| Total profile shift coefficient $x_1+x_2$ [mm] | 0.354 | -0.011 | -0.226 |
| Pinion profile shift coefficient $x_1$ [mm] | 0 | 0 | 0 |
| Wheel profile shift coefficient $x_2$ [mm] | 0.354 | -0.01 | -0.226 |

*Table 11 – Axial distances and profile shift coefficients*

### 2.9.3.3 GEAR DIMENSIONS

Dimensions of helical gears relate to chosen input parameters. The geometry of gears is calculated using formulas (24) – (29) and results are listed in the Table 12.

$$d = \frac{m_n \cdot z}{\cos ß} \tag{24}$$

$$d_f = d - 2 \cdot (h_a^* + c_a) \cdot m_n + 2 \cdot x_1 \cdot m_n \tag{25}$$

$$d_a = d + 2 \cdot h_a^* \cdot m_n + 2 \cdot x_1 \cdot m_n \tag{26}$$

$$d_b = d \cdot \cos(\alpha_t) \tag{27}$$

$$p_{bt} = \frac{\pi \cdot m_n \cdot \cos(\alpha_t)}{\cos ß} \tag{28}$$

$$m_t = \frac{m_n}{\cos ß} \tag{29}$$

|  | 1st speed | | 2nd speed | | Final drive | |
|---|---|---|---|---|---|---|
|  | Pinion | Wheel | Pinion | Wheel | Pinion | Wheel |
| Pitch circle diameter $d$ [mm] | 40.64 | 118.24 | 66.51 | 93.53 | 49.07 | 202.07 |
| Root circle diameter $d_f$ [mm] | 36.64 | 115.38 | 62.01 | 88.99 | 42.82 | 194.69 |
| Tip circle diameter $d_a$ [mm] | 43.82 | 122.56 | 70.11 | 97.09 | 54.06 | 205.93 |
| Base circle diameter $d_b$ [mm] | 37.47 | 109.01 | 61.31 | 86.23 | 45.24 | 186.29 |
| Trans. base pitch $p_{bt}$ [mm] | 5.35 | | 6.02 | | 8.36 | |
| Transverse modulus $m_t$ [mm] | 1.85 | | 2.08 | | 2.89 | |

*Table 12 – Gear dimensions*

#### 2.9.3.4 TOOTH CONTACT RATIO

The tooth contact ratio is one of the most important properties which determines if the gear pair will be working properly. Moreover, it plays a crucial role in the noise production of the transmission. For the proper functioning of the gear pair, the transverse contact ratio $\varepsilon_\alpha$ has to be greater than 1 [20]. The proposer of thesis set the minimal value of the total contact ratio to be $\varepsilon_\gamma \geq 3.5$. The contact ratios of all 3 gear pairs are listed in Table 13.

$$\varepsilon_\alpha = \frac{0{,}5 \cdot \sqrt{d_a^2 - d_b^2} + 0{,}5 \cdot \sqrt{d_a^2 - d_b^2} - a \cdot sin(\alpha_W)}{p_{bt}} \tag{30}$$

$$\varepsilon_\text{ß} = \frac{b \cdot \sin(\text{ß})}{\pi \cdot m_n} \tag{31}$$

$$\varepsilon_\gamma = \varepsilon_\alpha + \varepsilon_\text{ß} \tag{32}$$

|  | 1st speed | 2nd speed | Final drive |
|---|---|---|---|
| **Transverse contact ratio $\varepsilon_\alpha$ [-]** | 1.341 | 1.390 | 1.381 |
| **Overlap contact ratio $\varepsilon_\beta$ [-]** | 2.160 | 2.110 | 2.119 |
| **Total contact ratio $\varepsilon_\gamma$ [-]** | 3.501 | 3.5 | 3.5 |

*Table 13 – Tooth contact ratio*

### 2.9.4 DUTY CYCLE

The creation of an optimal duty cycle of the vehicle is a paramount task for the estimation of component service life. Yet the task is very complex because of the diversity of the vehicle usage. At the beginning of the process, the service life of the passenger car was set to 150 000 km. The keystone of the duty cycle was the software simulation of the WLTC cycle that should simulate real world driving. One mentioned cycle has length of 23.221 km, hence the car has to be able to execute approximately 6459 cycles. The total distance traveled with each gear engaged was determined from data on the usage of individual gears. The distance travelled with the engaged first gear is 76678.8 km and 73321.2 km with the second gear.

The next task was to estimate the average/reference transmission input torque and RPM. The torque usage in dependence with the RPM during one WLTC cycle for both first and second speed are shown in Figure 25, and Figure 26.
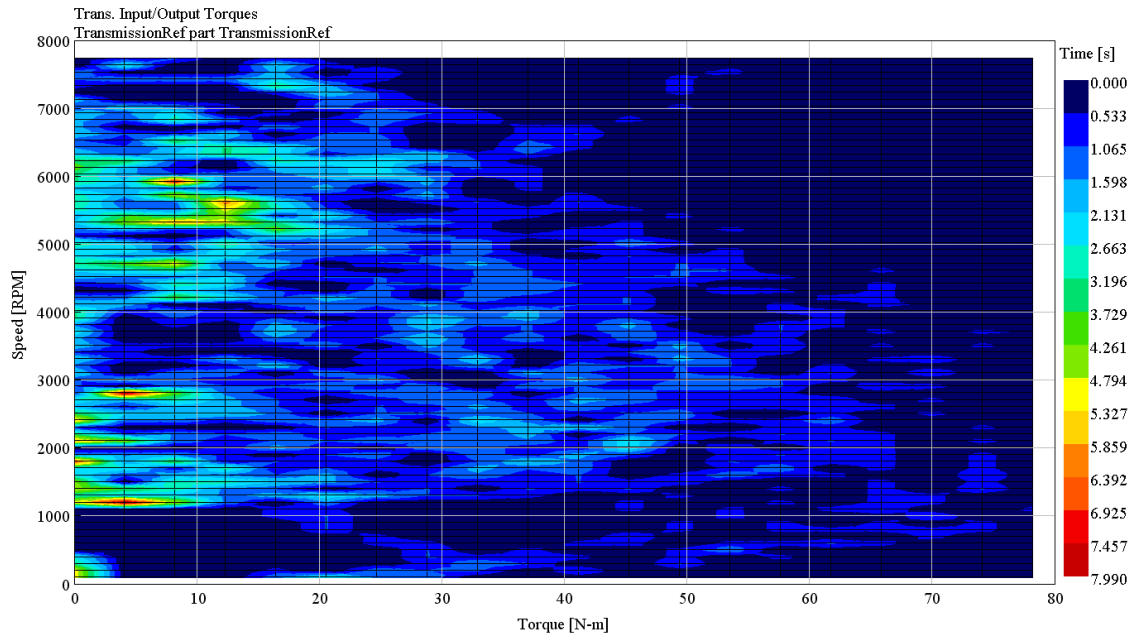
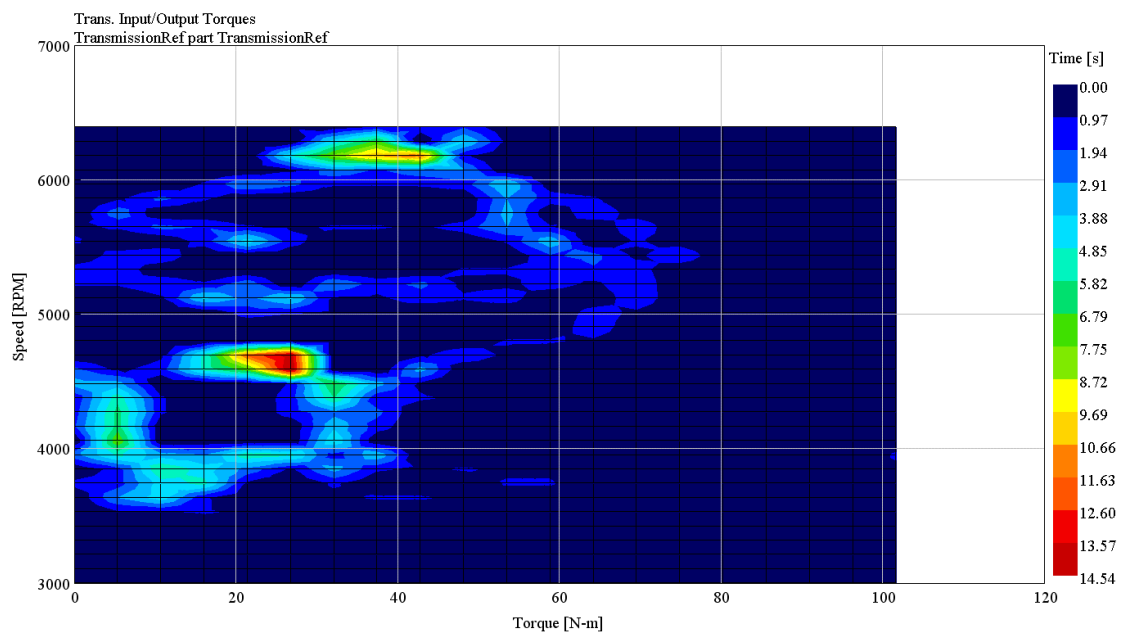*Figure 25 - The first gear torque usage proportional with the RPM during one WLTC*



*Figure 26 - The second gear torque usage proportional with the RPM during one WLTC*

3 parameters are necessary for the whole duty cycle – reference torque, reference RPM and reference time. It proceeds by selecting 2 of the parameters and calculating the third. In our case, reference torque and RPM were selected and reference time was calculated using an equation (33) utilizing data (torque vs. RPM vs. time) acquired from WLTC.

$$t_{ref} = \left(\frac{T}{T_{ref}}\right)^w \cdot \left(\frac{N}{N_{ref}}\right) \cdot t \qquad (33)$$

$T$       – Nominal torque [Nm]

$T_{ref}$   – Reference torque [Nm]

$t$   – Nominal time [h]

$t_{ref}$   – Reference time [h]

$N$   – Nominal RPM [RPM]

$N_{ref}$   – Reference RPM [RPM]

$w$   – Wöhler curve exponent / Equivalent load [-]

   – For bearings $w = 3$

   – For gear bending $w = 8.738$

   – For gear surface $w = 6.611$

Due to 3 different types of service lives, 3 duty cycles for each gear are necessary. In order to simulate maximal torque input, a fourth duty cycle is supplemented. The maximal motor torque in the highest possible RPM according to the motor performance map is used for the period of 3 hours. Duty cycles for each controlled parameter are listed in the tables 14 -17.

|  | 1st speed | 2nd speed |
|---|---|---|
| **Reference RPM [RPM]** | 4000 | 4000 |
| **Reference Torque [Nm]** | 100 | 100 |
| **Reference time [h]** | 59.01 | 66.83 |

*Table 14 – Duty cycle for bearings*

|  | 1st speed | 2nd speed |
|---|---|---|
| **Reference RPM [RPM]** | 4000 | 4000 |
| **Reference Torque [Nm]** | 100 | 100 |
| **Reference time [h]** | 2.42 | 10.35 |

*Table 15 – Duty cycle for gear bending*

|  | 1st speed | 2nd speed |
|---|---|---|
| **Reference RPM [RPM]** | 4000 | 4000 |
| **Reference Torque [Nm]** | 100 | 100 |
| **Reference time [h]** | 6.63 | 15.49 |

*Table 16 – Duty cycle for gear surface*

|  | 1st speed | 2nd speed |
|---|---|---|
| Reference RPM [RPM] | 4600 | 4600 |
| Reference Torque [Nm] | 250 | 250 |
| Reference time [h] | 3 | 3 |

*Table 17 – Duty cycle for maximal torque input*

## 2.9.5  MATERIAL OF GEARS

For the manufacturing of all gears, the low alloyed case hardened manganese – chromium steel 20MnCr5 (DIN 1.7147) that is suitable for carburizing is used. Shafts with built in pinions are also manufactured from the mentioned steel. The properties of the material after case hardening and carburizing to the hardness HRC 55 are listed in Table 18.

| Young modulus $E$ [MPa] | $2.06 \cdot 10^5$ |
|---|---|
| Tensile strength $R_m$  [MPa] | 900 |
| Yield strength $R_{p0.2}$ [MPa] | 650 |
| Endurance contact limit $\sigma_{Hlim}$  [MPa] | 1500 |
| Endurance bending limit $\sigma_{Flim}$  [MPa] | 460 |

*Table 18 – 20MnCr5 steel mechanical properties*

## 2.9.6  TORQUES AND RPM OF INDIVIDUAL SHAFTS

Torques and RPM of individual shafts are calculated using duty cycle parameters. Two types of loads are taken into account. Torques are calculated using formulas (34) – (35). Results are listed in the Table 19 and the Table 20.

$$M_i = M_{input} \cdot i_g \cdot n_g \tag{34}$$

$$N_i = N_{input} \cdot i_g \tag{35}$$

$M_i$       – Torques of individual shafts [Nm]

$M_{input}$       – Input torque [Nm]

$N_i$       – RPM of individual shafts [RPM]

$N_{input}$       – Input RPM [RPM]

$i_g$       – Gear ratio [-]

$\eta_g$       – efficiency of the gear [-], in helix gear $\eta_g = 0.98$

|  | 1st speed | | 2nd speed | |
|---|---|---|---|---|
|  | Torque [Nm] | RPM [RPM] | Torque [Nm] | RPM [RPM] |
| **1st input shaft** | 100 | 4000 | Not loaded | Not loaded |
| **2nd input shaft** | Not loaded | Not loaded | 100 | 4000 |
| **Output shaft** | 285.08 | 1375 | 137.78 | 2844.44 |
| **Final drive shaft** | 1150.48 | 333.93 | 556.03 | 690.79 |

*Table 19 – Shaft torques and RPM for the first duty cycle ($M_{input}$ = 100 Nm, $N_{input}$ = 4000 RPM)*

|  | 1st speed | | 2nd speed | |
|---|---|---|---|---|
|  | Torque [Nm] | RPM [RPM] | Torque [Nm] | RPM [RPM] |
| **1st input shaft** | 250 | 4600 | Not loaded | Not loaded |
| **2nd input shaft** | Not loaded | Not loaded | 250 | 4600 |
| **Output shaft** | 712.71 | 1581.25 | 344.47 | 3271.11 |
| **Final drive shaft** | 2876.24 | 384.08 | 1390.16 | 794.41 |

*Table 20 - Shaft torques and RPM for the second duty cycle ($M_{input}$ = 250 Nm, $N_{input}$ = 4600 RPM*

## 2.9.7 TEETH FORCES

Forces acting on tooth flanks are shown in the Figure 27. The magnitudes of the individual forces were determined by calculation from the torques acting on the individual shafts. Equations (36) – (38) were used for the computation of teeth forces. The results are listed in Table 21 and Table 22.

$$F_t = \frac{2 \cdot M_i}{d_i} \tag{36}$$

$$F_a = F_t \cdot tg(\text{ß}) \tag{37}$$

$$F_r = F_t \cdot \frac{tg(\alpha)}{\cos(\text{ß})} \tag{38}$$

47
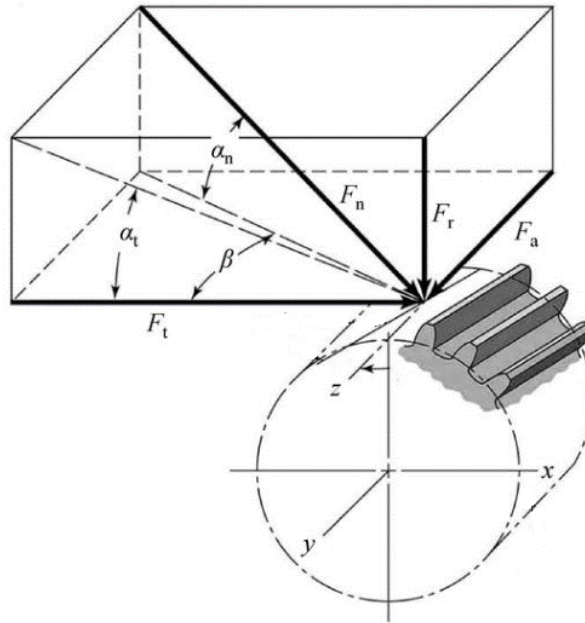
*Figure 27 – Forces acting on the tooth flank [26]*

| | 1st gear pair | 2nd gear pair | Final drive | |
|---|---|---|---|---|
| | | | 1st speed | 2nd speed |
| **Tangential force $F_t$ [N]** | 4887 | 3007 | 11619 | 5747 |
| **Axial force $F_a$ [N]** | 2821 | 1736 | 6708 | 3318 |
| **Radial force $F_r$ [N]** | 2054 | 1263 | 4883 | 2415 |

*Table 21 – Tooth forces for the first duty cycle ($M_{input}$ = 100 Nm, $N_{input}$ = 4000 RPM)*

| | 1st gear pair | 2nd gear pair | Final drive | |
|---|---|---|---|---|
| | | | 1st speed | 2nd speed |
| **Tangential force $F_t$ [N]** | 12301 | 7517 | 29547 | 14368 |
| **Axial force $F_a$ [N]** | 7102 | 4340 | 17058 | 8295 |
| **Radial force $F_r$ [N]** | 5169 | 3159 | 12417 | 6038 |

*Table 22 - Tooth forces for the second duty cycle ($M_{input}$ = 250 Nm, $N_{input}$ = 4600 RPM)*

## 2.9.8 GEAR LOAD CAPACITY

Gear load capacity was calculated using SABR/Gear software by Ricardo s.r.o. according to the standard ISO 6336: 2006 with gear accuracy grade of 8. The result is a safety factor for tooth root bending strength as well as a safety factor for the tooth contact stress. ISO application factor $K_a$ is set to be 1. Detailed data about safety factors are listed in Attachment 1.

### 2.9.8.1 SAFETY FACTOR FOR CONTACT STRESS $S_H$

The load for the calculation of the contact safety factor is based on the mean circumferential force acting on the tooth flank. The eventual safety factor is dependent on the material properties of the gear and is computed using formulas below. The gear load was based on the duty cycle for gear surface stated in Chapter 2.9.4. The achieved values are listed in Table 23.

$$\sigma_H = Z_H \cdot Z_E \cdot Z_{B.D} \cdot Z_\epsilon \cdot Z_\beta \cdot \sqrt{\frac{(i+1) \cdot F_t}{i \cdot b_w \cdot d}} \tag{39}$$

$$S_H = \frac{\sigma_{Hlim} \cdot Z_R \cdot Z_{NT} \cdot Z_L \cdot Z_V \cdot Z_W \cdot Z_X}{\sigma_H \sqrt{Z_B^2 \cdot K_A \cdot K_V \cdot K_{H\alpha} \cdot K_{H\beta}}} \tag{40}$$

| | 1st gear pair | | 2nd gear pair | | Final drive | | | |
| | | | | | 1st speed | | 2nd speed | |
| | pinion | wheel | pinion | wheel | pin. | wh. | pin. | wh. |
|---|---|---|---|---|---|---|---|---|
| **Endurance contact limit $\sigma_{Hlim}$ [MPa]** | 1500 | | | | | | | |
| **Contact stress $\sigma_H$ [Mpa]** | 1283 | | 982 | | 1291 | | 1041 | |
| **Safety factor $S_H$ [N]** | 1.44 | 1.59 | 1.75 | 1.81 | 1.58 | 1.81 | 1.69 | 1.93 |

*Table 23 – Contact stress and safety factor for the contact stress $S_H$*

### 2.9.8.2 SAFETY FACTOR FOR BENDING STRENGTH $S_F$

When calculating the bending safety factor we must imagine the tooth as a cantilevered beam, loaded by a static solitary force F acting on the tooth flank. The gear load was based on the duty cycle for gear bending stated in Chapter 2.9.4. The achieved values are calculated using equations (41) – (42) and listed in Table 24.

$$\sigma_F = \frac{F_t \cdot K_A \cdot K_V \cdot K_{F\alpha} \cdot K_{F\beta}}{b_w \cdot m_n} \cdot Y_{Fa} \cdot Y_{Sa} \cdot Y_\epsilon \cdot Y_\beta \tag{41}$$

$$S_F = \frac{\sigma_{Flim} \cdot Y_{ST} \cdot Y_{NT} \cdot Y_{\delta,relT} \cdot Y_X}{\sigma_F} \tag{42}$$

| | 1st gear pair | | 2nd gear pair | | Final drive | | | |
|---|---|---|---|---|---|---|---|---|
| | | | | | 1st speed | | 2nd speed | |
| | pinion | wheel | pinion | wheel | pin. | wh. | pin. | wh. |
| Endurance bending limit $\sigma_{Flim}$ [MPa] | 460 | | | | | | | |
| Bending stress $\sigma_F$ [Mpa] | 384 | 370 | 220 | 242 | 295 | 302 | 192 | 197 |
| Safety factor $S_F$ [N] | 2.74 | 3.41 | 4.07 | 3.87 | 4.03 | 4.78 | 4.83 | 5.65 |

*Table 24 - Bending stress and safety factor for the bending stress $S_H$*

## 2.9.9 DESIGN OF SHAFTS

### 2.9.9.1 SHAFT DIMENSIONS

The preliminary dimensioning of transmission shafts is based on the magnitude of the applied torque and material permissible torque stress according to the formula (43) (for shafts without bore). However, the second input shaft has to be hollow (the first input shaft is located inside it) due to the coupling of both input shafts with the dual clutch. The bore of the hollow shaft was chosen to provide sufficient clearance for the rotating first input shaft as well as to support needle bearing of the mentioned shaft.

$$d = \sqrt[3]{\frac{16 \cdot M_i}{\pi \cdot \tau_D}} \qquad (43)$$

The proposed diameters and lengths of the shafts are shown in the figures below. During the proposal process, it was important to consider the bearings' inner ring diameters that are usually graded by 5 mm. The design of the final drive assembly was based on the final drive provided by Ricardo s.r.o.

Designed shafts subsequently undergo static and dynamic strength control that is discussed in the following chapters.
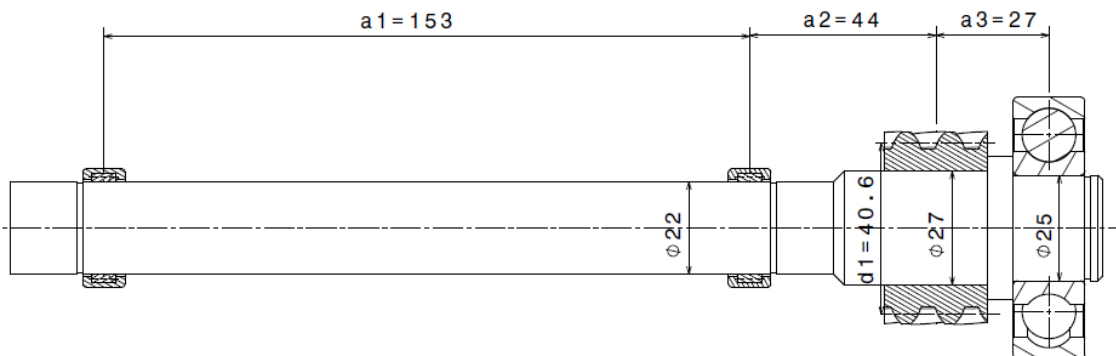


*Figure 28 – The first input shaft dimensions*
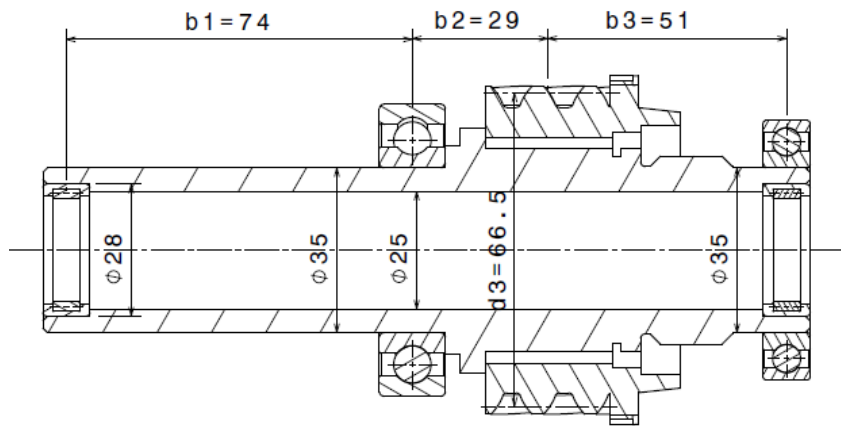
*Figure 29 – The second (holow) input shaft dimensions*
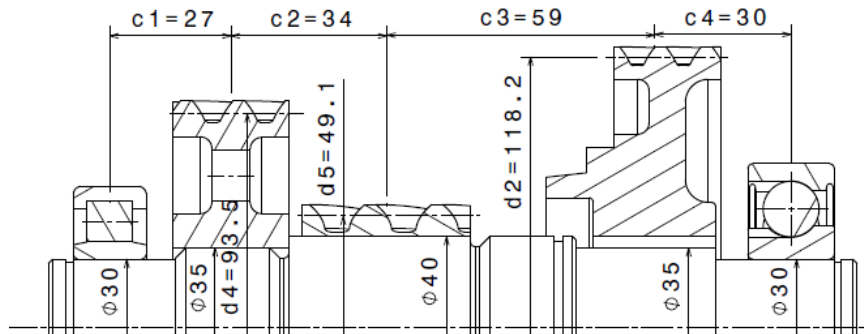


*Figure 30 – Output shaft (counter shaft) dimensions*
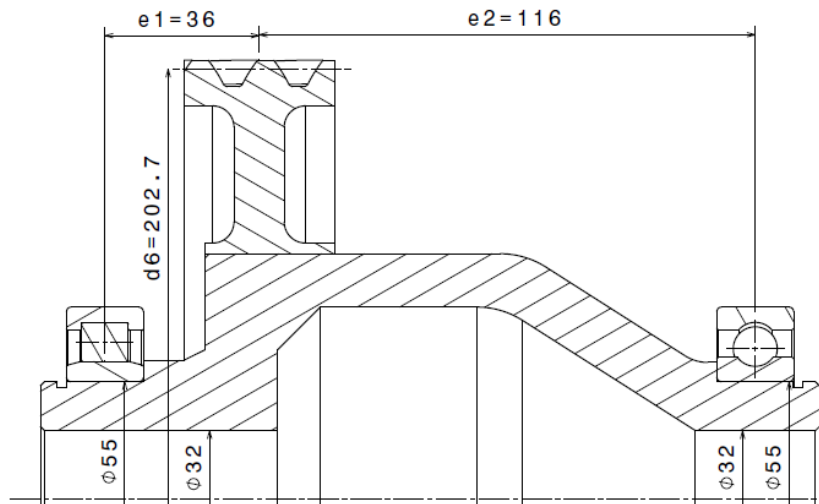


*Figure 31 – Differential assembly dimensions*

## 2.9.9.2    SHAFT CONFIGURATION

In contrast with heavy industrial transmissions, individual shafts of vehicle transmission are not usually situated in the same plane due to the more compact dimensions and beneficial force distribution. The side view of the shaft configuration can be seen in Figure 32.
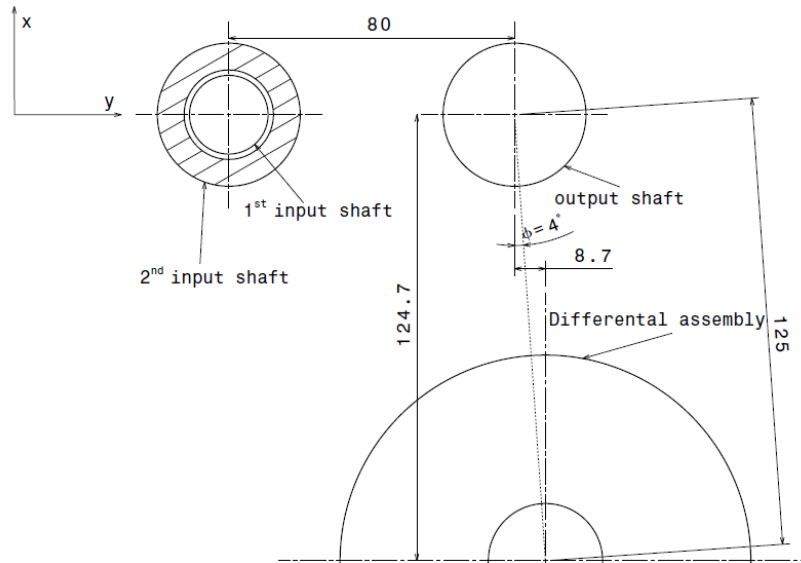
*Figure 32 – Shafts configuration*

## 2.9.9.3 REACTION FORCES IN BEARINGS

The calculation of reaction forces in bearings consists of analytical computation of a statically determined beam in two mutually perpendicular planes. The results are calculated using Ricardo's SABR/Gear software.

**THE FIRST INPUT SHAFT:**

The first input shaft is loaded with the torque Mi from the electric motor, bending moment from the reaction forces in bearings and by the force F1 [Fa12 (z – direction), Fr12 (y – direction), Ft12 (x – direction)] in the gearing as can be seen in Figure 33. The right ball bearing (RC) retains axial forces. The shaft is loaded by two types of loads according to 2 duty cycles applied – the duty cycle for bearings and the duty cycle for the maximal torque input. The magnitudes of the forces are calculated using the equations below and the results are summarized in Table 25 and Table 26.
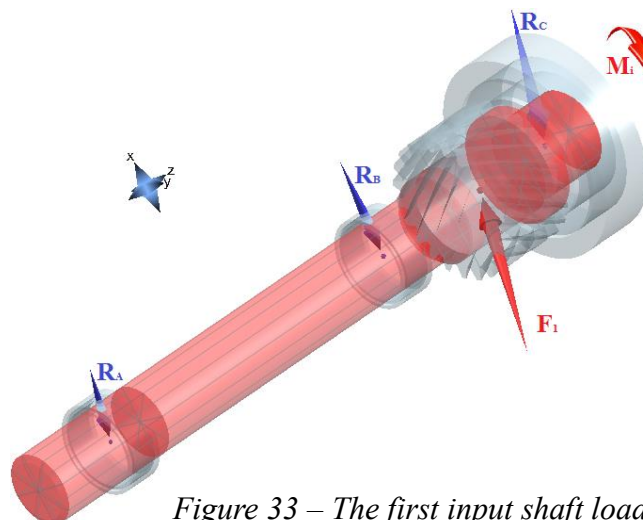


*Figure 33 – The first input shaft loads*

Plane XZ:

$$\sum F_{ix} = 0: \ R_{Cx} - F_{t12} + R_{Bx} + R_{Ax} = 0 \tag{44}$$

$$\sum F_{iz} = 0: \ R_{Cz} = F_{a12} \tag{45}$$

$$\sum M_{Cy} = 0: \ R_{Ax} \cdot (a_1 + a_2 + a_3) + R_{Bx} \cdot (a_2 + a_3) + F_{a12} \cdot \frac{d_1}{2} - F_{t12} \cdot a_3 = 0 \tag{46}$$

$$\sum M_{By} = 0 : R_{Ax} \cdot a_1 - R_{Cx} \cdot (a_1 + a_2 + a_3) + F_{a12} \cdot \frac{d_1}{2} + F_{t12} \cdot (a_2 + a_3) = 0 \tag{47}$$

Plane YZ:

$$\sum F_{iy} = 0: \ R_{Cy} - F_{r12} + R_{By} + R_{Ay} = 0 \tag{48}$$

$$\sum M_{Cx} = 0: \ R_{Ay} \cdot (a_1 + a_2 + a_3) + R_{By} \cdot (a_2 + a_3) + F_{a12} \cdot \frac{d_1}{2} - F_{r12} \cdot a_3 = 0 \tag{49}$$

$$\sum M_{Bx} = 0 : R_{Ay} \cdot a_1 - R_{Cy} \cdot (a_1 + a_2 + a_3) + F_{a12} \cdot \frac{d_1}{2} + F_{r12} \cdot (a_2 + a_3) = 0 \tag{50}$$

| $R_{Ax}$ [N] | $R_{Ay}$ [N] | $R_{Az}$ [N] | $R_{Bx}$ [N] | $R_{By}$ [N] | $R_{Bz}$ [N] | $R_{Cx}$ [N] | $R_{Cy}$ [N] | $R_{Cz}$ [N] |
|---|---|---|---|---|---|---|---|---|
| -160 | -53 | 0 | -1126 | -89 | 0 | -3660 | 2290 | -2841 |

*Table 25 – Reaction forces in the first input shaft bearings according to the duty cycle for bearings*

| $R_{Ax}$ [N] | $R_{Ay}$ [N] | $R_{Az}$ [N] | $R_{Bx}$ [N] | $R_{By}$ [N] | $R_{Bz}$ [N] | $R_{Cx}$ [N] | $R_{Cy}$ [N] | $R_{Cz}$ [N] |
|---|---|---|---|---|---|---|---|---|
| -196 | -125 | 0 | -3200 | -350 | 0 | -8821 | 5844 | -7102 |

*Table 26 - Reaction forces in the first input shaft bearings according to the duty cycle of the maximal torque input*

**THE SECOND INPUT SHAFT:**

When the second gear is engaged the second input shaft is loaded with the torque Mi generated in the gearing, bending moment from the reaction forces in bearings and by the force F2 (Fa34, Fr34, Ft34) in the gearing as can be seen in Figure 34. In contrast with the first input shaft – the second (hollow) one retains forces from the needle bearings when the first gear is engaged as can be seen in Figure 35. The left ball bearing retains axial forces. The small amount of load is also transferred to the needle bearings located on the first input shaft. The shaft is loaded with 4 types of loads (the first and the second gear) according to 2 duty cycles applied – the duty cycle for the bearings and the duty cycle of the maximal torque input. The magnitudes of the forces are calculated using equations (51) - (63) and the results are summarized in the tables below.
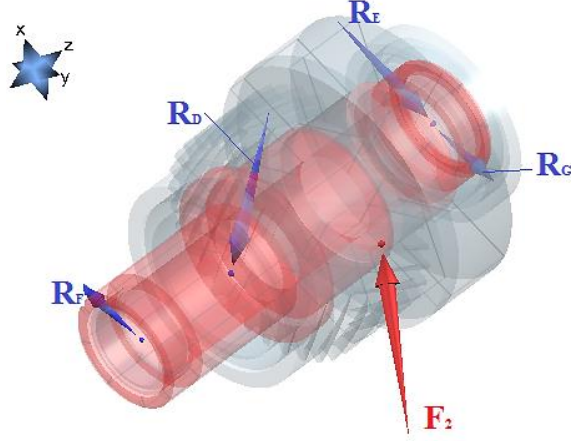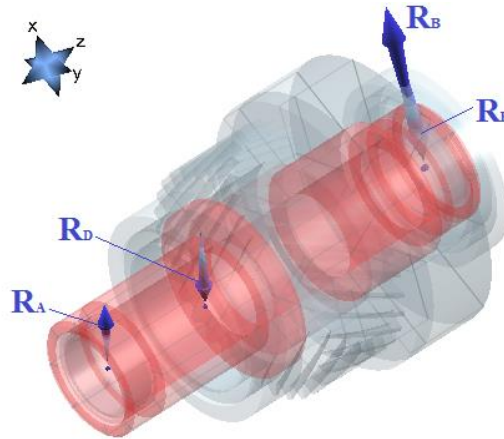
*Figure 34 - The second input shaft loads during second gear*

Plane XZ:

$$\sum F_{ix} = 0:\ R_{Dx} - F_{t34} + R_{Ex} + R_{Gx} - R_{Fx} = 0 \tag{51}$$

$$\sum F_{iz} = 0:\ R_{Dz} = F_{a34} \tag{52}$$

$$\sum M_{Dy} = 0:\ -R_{Fx} \cdot b_1 + F_{t34} \cdot b_2 + F_{a34} \cdot \frac{d_3}{2} - (R_{Gx} + R_{Ex}) \cdot (b_3 + b_2) = 0 \tag{53}$$

$$\sum M_{E/Gy} = 0:\ -R_{Fx} \cdot (b_3 + b_2 + b_1) - R_{Dx} \cdot (b_3 + b_2) + F_{a34} \cdot \frac{d_3}{2} - F_{t12} \cdot b_3 = 0 \tag{54}$$

$$\sum M_{Fy} = 0:\ -R_{Dx} \cdot b_1 + F_{t34} \cdot (b_2 + b_1) + F_{a34} \cdot \frac{d_3}{2} -$$
$$(R_{Gx} + R_{Ex}) \cdot (b_3 + b_2 + b_1) = 0 \tag{55}$$

Plane YZ:

$$\sum F_{iy} = 0:\ -R_{Fy} - F_{r34} + R_{Dy} + R_{Gy} + R_{Ey} = 0 \tag{56}$$

$$\sum M_{Dx} = 0:\ -R_{Fy} \cdot b_1 - (R_{Gx} + R_{Ex}) \cdot (b_3 + b_2) + F_{a34} \cdot \frac{d_3}{2} + F_{r34} \cdot b_2 = 0 \tag{57}$$

$$\sum M_{E/Gx} = 0:\ -R_{Fy} \cdot (b_3 + b_2 + b_1) + R_{Dy} \cdot (b_3 + b_2) + F_{a34} \cdot \frac{d_3}{2} + F_{r34} \cdot b_3 = 0 \tag{58}$$

$$\sum M_{Fx} = 0:\ -R_{Dy} \cdot b_1 + F_{r34} \cdot (b_2 + b_1) + F_{a34} \cdot \frac{d_3}{2} -$$
$$(R_{Gx} + R_{Ex}) \cdot (b_3 + b_2 + b_1) = 0 \tag{59}$$

| $R_{Dx}$ [N] | -1856 |
|---|---|
| $R_{Dy}$ [N] | 109 |
| $R_{Dz}$ [N] | -1736 |
| $R_{Ex}$ [N] | -1152 |
| $R_{Ey}$ [N] | 1153 |
| $R_{Ez}$ [N] | 0 |

| $R_{Fx}$ [N] | 0 |
|---|---|
| $R_{Fy}$ [N] | 0 |
| $R_{Fz}$ [N] | 0 |
| $R_{Gx}$ [N] | 0 |
| $R_{Gy}$ [N] | 0 |
| $R_{Gz}$ [N] | 0 |

*Table 27 – Reaction forces in the second input shaft bearings according to the duty cycle for bearings, when the second gear is engaged*

| $R_{Dx}$ [N] | -4596 |
|---|---|
| $R_{Dy}$ [N] | 314 |
| $R_{Dz}$ [N] | -4340 |
| $R_{Ex}$ [N] | -2894 |
| $R_{Ey}$ [N] | 2803 |
| $R_{Ez}$ [N] | 0 |

| $R_{Fx}$ [N] | 18 |
|---|---|
| $R_{Fy}$ [N] | -23 |
| $R_{Fz}$ [N] | 0 |
| $R_{Gx}$ [N] | -47 |
| $R_{Gy}$ [N] | 60 |
| $R_{Gz}$ [N] | 0 |

*Table 28 - Reaction forces in the second input shaft bearings according to the duty cycle of the maximal torque input, when the second gear is engaged*



*Figure 35 - The second input shaft loads during first gear*

Plane XZ:

$$\sum F_{ix} = 0: \ R_{Ax} - R_{Dx} - R_{Ex} + R_{Bx} = 0 \tag{60}$$

$$\sum M_{Ey} = 0: \ R_{Ax} \cdot (b_3 + b_2 + b_1) R_{Ax} \cdot (b_3 + b_2 + b_1) = 0 \tag{61}$$

Plane YZ:

$$\sum F_{iy} = 0: \ R_{Ay} - R_{Dy} + R_{By} - R_{Ey} = 0 \tag{62}$$

$$\sum M_{Ex} = 0: \quad R_{Ay} \cdot (b_3 + b_2 + b_1) - R_{Ax} \cdot (b_3 + b_2) = 0 \tag{63}$$

| $R_{Dx}$ [N] | $R_{Dy}$ [N] | $R_{Dz}$ [N] | $R_{Ex}$ [N] | $R_{Ey}$ [N] | $R_{Ez}$ [N] |
|---|---|---|---|---|---|
| -240 | -77 | 0 | -1046 | -65 | 0 |

*Table 29 – Reaction forces in the second input shaft bearings according to the duty cycle for bearings, when the first gear is engaged*

| $R_{Dx}$ [N] | $R_{Dy}$ [N] | $R_{Dz}$ [N] | $R_{Ex}$ [N] | $R_{Ey}$ [N] | $R_{Ez}$ [N] |
|---|---|---|---|---|---|
| 10 | -77 | 0 | -1046 | -65 | 0 |

*Table 30- Reaction forces in the second input shaft bearings according to the duty cycle of the maximal torque input, when the first gear is engaged*

## THE OUTPUT SHAFT (COUNTERSHAFT)

The output shaft is loaded with the torque Mi from the gearing, bending moment from the reaction forces in bearings and by gear forces F1 (Fa12, Fr12, Ft12) – the first gear pair, F2 (Fa34, Fr34, Ft34) – the second gear pair and F3 (F3x, F3y, F3z) - final drive as can be seen in the Figure 36. Both wheels have right handed helix. The final drive pinion has left helix hand in order to minimalize axial load in the right ball bearing. The shaft is loaded with four types of loads according to 2 duty cycles applied – the duty cycle for the bearings and the duty cycle for the maximal torque input. Magnitudes of the forces are calculated using equations (67) - (76) and the results are summarized in the tables below.
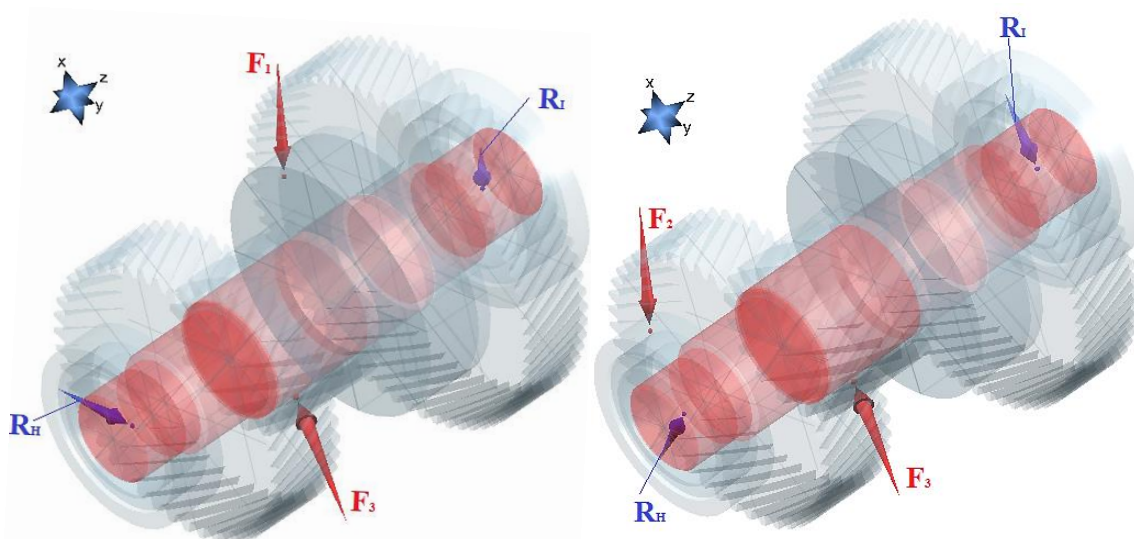


*Figure 36 - Output shaft loads. First gear engaged (left), Second gear engaged (right).*

In the beginning of the calculations, it is important to take into account that the differential assembly does not lay on the plane ZY, but it is offset in the direction of the

x axis. Due to that reason, tooth contact between the pinion and the wheel occurs in the plane of offset from the plane XY by the angle $\varphi = 4°$ according to the Figure 32. Hence, we cannot assume that $F_{axial}$ acts in the z direction, $F_{radial}$ acts in y direction and $F_{tangential}$ acts in x direction as in the previous cases. For the determination of individual forces, equations (64)-(71) are used.

$$F_{3x} = F_{r56} \cdot \cos(\varphi) - F_{t56} \cdot \sin(\varphi) \tag{64}$$

$$F_{3y} = F_{t56} \cdot \cos(\varphi) + F_{r56} \cdot \sin(\varphi) \tag{65}$$

$$F_{3z} = F_{a56} \tag{66}$$

The first gear engaged:

Plane XZ:

$$\sum F_{ix} = 0: \; -R_{Hx} + F_{3x} - F_{t12} + R_{Ix} = 0 \tag{67}$$

$$\sum F_{iz} = 0: \; R_{Iz} + F_{a12} - F_{3z} = 0 \tag{68}$$

$$\sum M_{Iy} = 0: -R_{Hx} \cdot (c_1 + c_2 + c_3 + c_4) - F_{3z} \cdot \frac{d_5}{2} + F_{3x} \cdot (c_3 + c_4) - F_{t12} \cdot c_4 -$$

$$F_{a12} \cdot \frac{d_2}{2} = 0 \tag{69}$$

Plane YZ:

$$\sum F_{iy} = 0: \; R_{Hy} - F_{3y} + F_{r12} + R_{Iy} = 0 \tag{70}$$

$$\sum M_{Ix} = 0: R_{Hy} \cdot (c_1 + c_2 + c_3 + c_4) + F_{3z} \cdot \frac{d_5}{2} - F_{3y} \cdot (c_3 + c_4) + F_{r12} \cdot c_4 -$$

$$F_{a12} \cdot \frac{d_2}{2} = 0 \tag{71}$$

| $R_{Hx}$ [N] | $R_{Hy}$ [N] | $R_{Hz}$ [N] | $R_{Ix}$ [N] | $R_{Iy}$ [N] | $R_{Iz}$ [N] |
|---|---|---|---|---|---|
| -368 | 5280 | 0 | 1239 | 4789 | -4005 |

*Table 31- Reaction forces in the output shaft bearings according to the duty cycle for bearings, when the first gear is engaged*

| $R_{Hx}$ [N] | $R_{Hy}$ [N] | $R_{Hz}$ [N] | $R_{Ix}$ [N] | $R_{Iy}$ [N] | $R_{Iz}$ [N] |
|---|---|---|---|---|---|
| -947 | 13033 | 0 | 3125 | 12141 | -10010 |

*Table 32- Reaction forces in the output shaft bearings according to the duty cycle of the maximal torque input, when the first gear is engaged*

The second gear engaged:

Plane XZ:

$$\sum F_{ix} = 0: \; +R_{Hx} + F_{3x} - F_{t34} - R_{Ix} = 0 \tag{72}$$

$$\sum F_{iz} = 0: \; R_{Iz} + F_{a34} - F_{3z} = 0 \tag{73}$$

$$\sum M_{Iy} = 0: R_{Hx} \cdot (c_1 + c_2 + c_3 + c_4) - F_{3z} \cdot \frac{d_5}{2} + F_{3x} \cdot (c_3 + c_4) - F_{t34} \cdot (c_2 + c_3 +$$

$$c_4) - F_{a34} \cdot \frac{d_4}{2} = 0 \tag{74}$$

Plane YZ:

$$\sum F_{iy} = 0: \ R_{Hy} - F_{3y} + F_{r34} + R_{Iy} = 0 \tag{75}$$

$$\sum M_{Ix} = 0: R_{Hy} \cdot (c_1 + c_2 + c_3 + c_4) + F_{3z} \cdot \frac{d_5}{2} - F_{3y} \cdot (c_3 + c_4) + F_{r34} \cdot (c_2 + c_3 +$$

$$c_4) - F_{a34} \cdot \frac{d_4}{2} = 0 \tag{76}$$

| $R_{Hx}$ [N] | $R_{Hy}$ [N] | $R_{Hz}$ [N] | $R_{Ix}$ [N] | $R_{Iy}$ [N] | $R_{Iz}$ [N] |
|---|---|---|---|---|---|
| 1891 | 1721 | 0 | -824 | 2923 | -1573 |

*Table 33 - Reaction forces in the output shaft bearings according to the duty cycle for bearings, when the second gear is engaged*

| $R_{Hx}$ [N] | $R_{Hy}$ [N] | $R_{Hz}$ [N] | $R_{Ix}$ [N] | $R_{Iy}$ [N] | $R_{Iz}$ [N] |
|---|---|---|---|---|---|
| 1891 | 1721 | 0 | -824 | 2923 | -1573 |

*Table 34 - Reaction forces in the output shaft bearings according to the duty cycle of the maximal torque input, when the second gear is engaged*

**FINAL DRIVE SHAFT:**

The final drive shaft is loaded with the torque Mi from the gear mesh, bending moment from the reaction forces in bearings and by gear force F3 (F3x, F3y, F3z) in accordance with equations (64) - (66). The right ball bearing (RK) retains axial forces. The shaft is loaded with two types of loads according to 2 duty cycles applied – the duty cycle for the bearings and the duty cycle of the maximal torque input. Magnitudes of the forces are calculated using equations below and the results are summarized in Table 35.
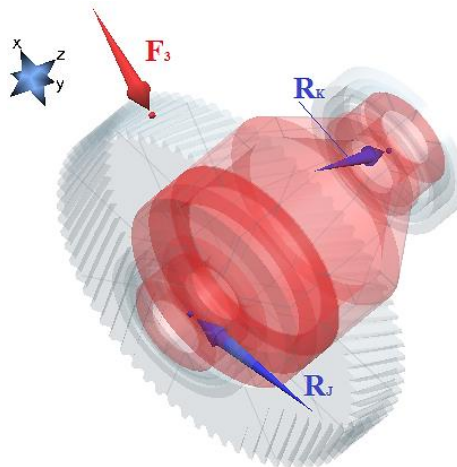


*Figure 37 – Final drive shaft loads*

Plane XZ:

$$\sum F_{ix} = 0: \ R_{Jx} - F_{3x} - R_{Kx} = 0 \tag{77}$$

$$\sum F_{iz} = 0: \ R_{Kz} - F_{3z} = 0 \tag{78}$$

$$\sum M_{Ky} = 0: R_{Jx} \cdot (e_1 + e_2) - F_{3z} \cdot \frac{d_6}{2} + F_{3x} \cdot e_2 = 0 \tag{79}$$

Plane YZ:

$$\sum F_{iy} = 0: \ -R_{Jy} + F_{3y} - R_{Ky} = 0 \tag{80}$$

$$\sum M_{Kx} = 0: -R_{Jy} \cdot (e_1 + e_2) - F_{3z} \cdot \frac{d_6}{2} + F_{3y} \cdot e_2 = 0 \tag{81}$$

| | $R_{Jx}$ [N] | $R_{Jy}$ [N] | $R_{Jz}$ [N] | $R_{Kx}$ [N] | $R_{Ky}$ [N] | $R_{Kz}$ [N] |
|---|---|---|---|---|---|---|
| **1st gear bearings** | 7473 | -10170 | 0 | -3757 | -2047 | 6846 |
| **1st gear max. torque** | 18528 | -25491 | 0 | -8490 | -5052 | 17112 |
| **2nd gear bearings** | 3632 | -4906 | 0 | -1691 | -1000 | 3309 |
| **2nd gear max. torque** | 9017 | -12298 | 0 | -4164 | -2467 | 8272 |

*Table 35 - Reaction forces in the final drive shaft bearings*

## 2.9.9.4 SHAFT STRENGTH CONTROL

Loads acting on the individual shafts were described in the chapter above. Shaft strength control consists of the comparison of calculated stress values $\sigma_{red}$ with the highest recommended stress value to prevent shafts from undesirable deflection (subsequent gear misalignment) $\sigma_D = 500MPa$. Ricardo´s SABR/Gear software was used for the calculation of shaft stress. Each shaft was controlled by two criteria for the ductile material - von Mises yield criterion (82) and Tresca yield criterion (83). The duty cycle of the maximal torque input was used. Shaft stress concentrations are shown in the figures below.

$$\sigma_{red_{Mises}} = \frac{\sqrt{2}}{2} \cdot \sqrt{\left(\sigma_x - \sigma_y\right)^2 + \left(\sigma_y - \sigma_z\right)^2 + (\sigma_z - \sigma_x)^2 + 6 \cdot \tau_x^2 \cdot \tau_y^2 \cdot \tau_z^2} \tag{82}$$

$$\sigma_{red_{Tresca}} = \sigma_1 - \sigma_3 = \sigma_{max} - \sigma_{min} \tag{83}$$

**THE FIRST INPUT SHAFT:**
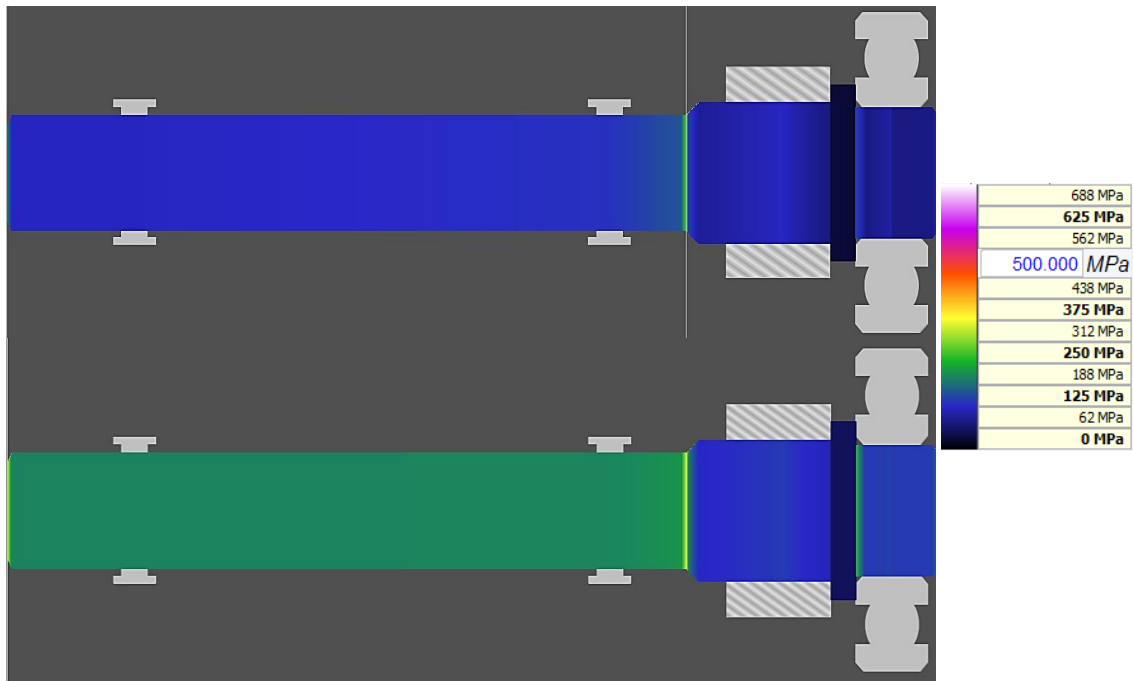


*Figure 38 - Stress in the first input shaft. Tresca criterion above, Von Mises criterion below.*

According to Figure 38, the highest stress concentration is located between the pinion and the middle needle bearing, where the shaft diameter is changing. Peak stress values are:

$$\sigma_{red1_{Mises}} = 378\ MPa$$

$$\sigma_{red1_{Tresca}} = 291\ MPa$$

The first input shaft stress, when the first gear is engaged is within the limit of the material. The safety factor of the shaft following the more strict – von Mises strength criterion is $S_{Mises} = 1.32$.

**THE SECOND INPUT SHAFT:**
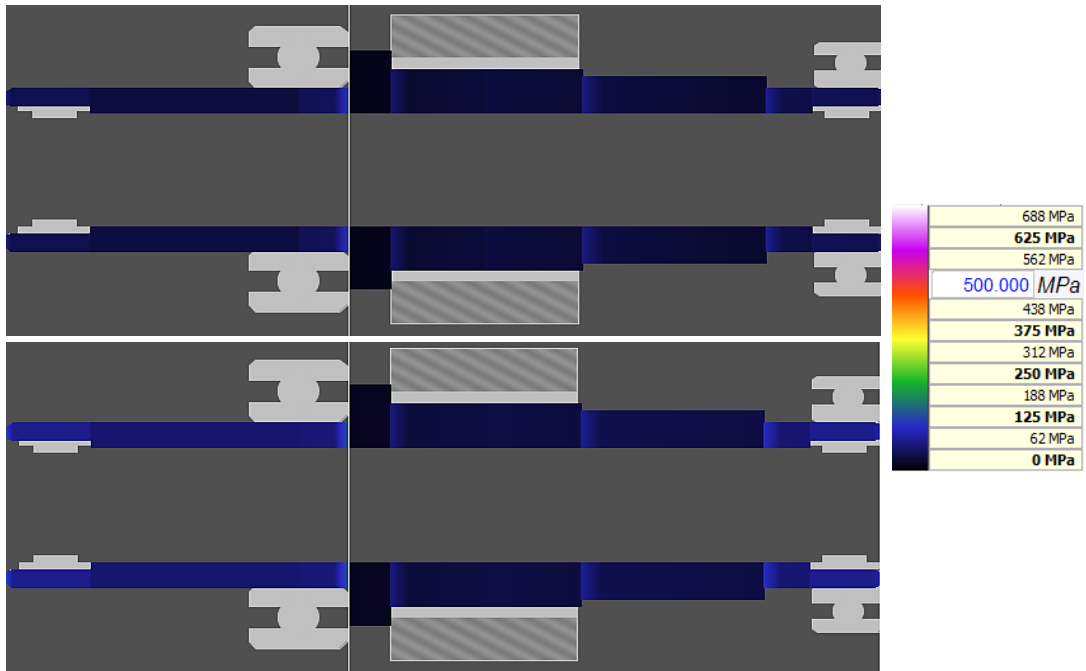


*Figure 39 - Stress in the second input shaft. Tresca criterion above, Von Mises criterion below.*

The figure above shows that the highest stress concentration lays on the right side of the left ball bearing. Peak stress values are:

$$\sigma_{red2_{Mises}} = 174 \ MPa$$

$$\sigma_{red2_{Tresca}} = 141 \ MPa$$

The second input shaft stress, when the second gear is engaged is within the limit of the material. The safety factor of the shaft $S_{Mises} = 2.87$

**THE OUTPUT SHAFT (COUNTERSHAFT):**
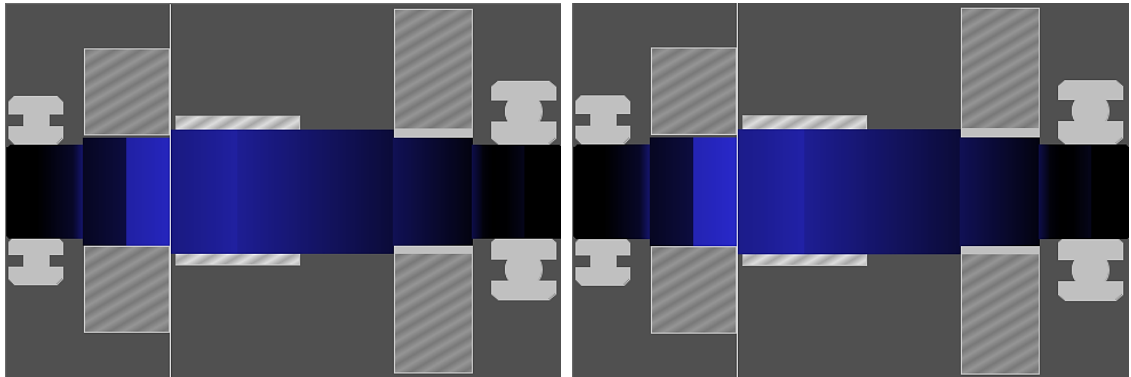


*Figure 40 - Stress in the output shaft. the first gear engaged. Tresca criterion (left),*
*Von Mises criterion (right).*
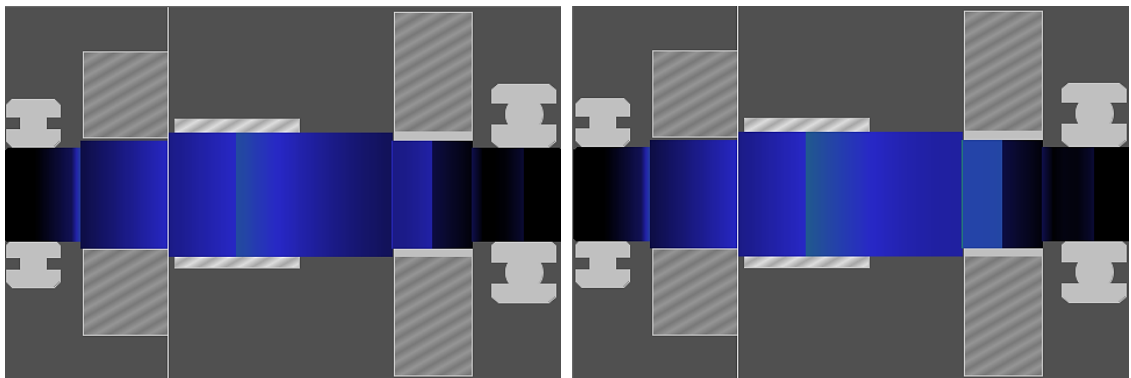


*Figure 41 - Stress in the output shaft. the second gear engaged. Tresca criterion (left),*
*Von Mises criterion (right).*

According to the figures above, the highest stress concentration is located between the second gear wheel and the final drive pinion. Peak stress values for the first gear are:

$$\sigma_{red3_{Mises}} = 288 \ MPa$$

$$\sigma_{red3_{Tresca}} = 288 \ MPa$$

And for the second gear:

$$\sigma_{red3_{Mises}} = 275 \ MPa$$

$$\sigma_{red3_{Tresca}} = 264 \ MPa$$

The output shaft stress is within the limit of the material yield strength. The minimal safety factor (for the first gear) following the more strict - von Mises strength criterion is $S_{Mises} = 1.74$

## FINAL DRIVE SHAFT:

The figures above show that the highest stress concentration lays on the left side of the right ball bearing.
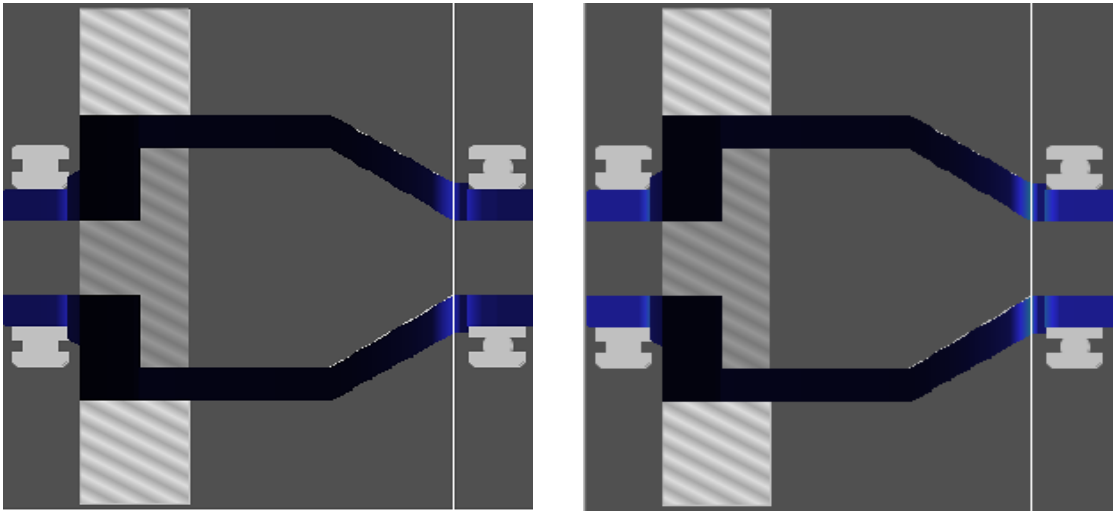


*Figure 42 - Stress in the final drive shaft. The first gear engaged. Tresca criterion (left), Von Mises criterion (right).*
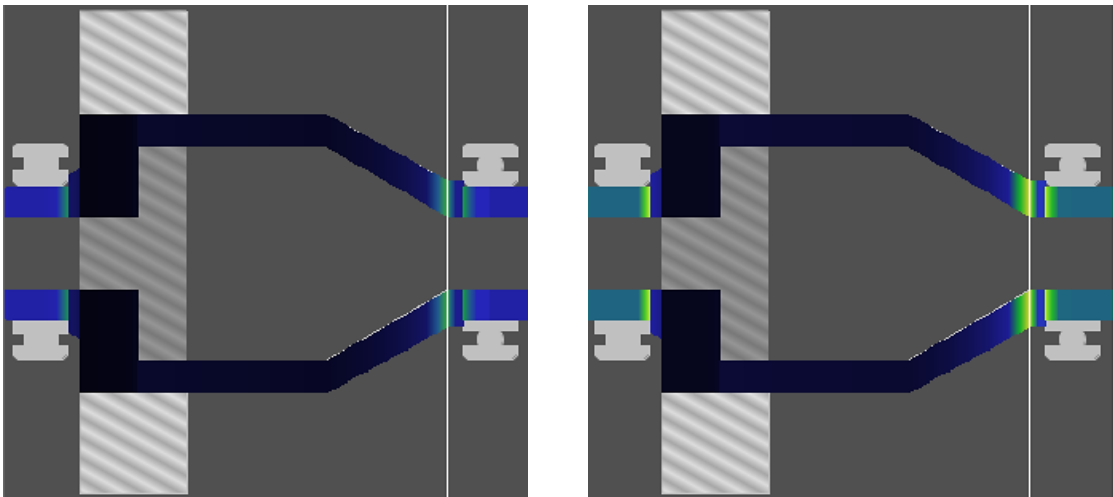


*Figure 43 - Stress in the final drive shaft. The first gear engaged. Tresca criterion (left), Von Mises criterion (right).*

Peak stress values for the first gear are:

$$\sigma_{red4_{Mises}} = 401 \; MPa$$

$$\sigma_{red4_{Tresca}} = 271 \; MPa$$

And for the second gear:

$$\sigma_{red4_{Mises}} = 194 \; MPa$$

$$\sigma_{red4_{Tresca}} = 130 \; MPa$$

The final drive shaft stress is within the limit of the material yield strength. Safety factor $S_{Mises} = 1.25$.

## 2.9.10 BEARINGS CALCULATION

### 2.9.10.1 CHOICE OF BEARINGS

Gearbox and final drive shafts as well as the second gear pinion and the first gear wheel are rotating in bearings. For this purpose, the roller, ball and needle bearing from the SKF were used due to its common utilization in this kind of application. The chosen bearings are listed in Table 36 below. The letters in the brackets assign bearings to shaft reaction forces calculated in the 2.9.9.3.

|  | **Left Bearing** | **Middle bearing** | **Right Bearing** | **Gear bearing** |
|---|---|---|---|---|
| **1st input shaft** | HK 2210 (A) (needle) | HK 2210 (B) (needle) | 6305ETN9 (C) (ball) | - |
| **2nd input shaft** | 6007 (D) (ball) | - | 61907 (E) (ball) | K43x48x27 (needle) |
| **Output shaft** | NJ206 (H) (roller) | - | SKF_306 (I) (ball) | K35x40x27 (needle) |
| **Final drive** | NU1011ECP (J) (roller) | - | 6011 (K) (ball) | - |

*Table 36 - Bearings*

### 2.9.10.2 BEARINGS CONTROL

Each bearing is controlled considering a combination of duty cycle for bearings and duty cycle of maximal torque input with the parameters shown in Table 14 and Table 17 in accordance with the standard - ISO 281. Calculations of bearing life are based on the dynamic equivalent bearing load, which includes radial and axial load and it is given by the formula (85)[27].

$$F_R = \sqrt{A_x^2 + A_y^2} \qquad (84)$$

$$P = X \cdot F_R + Y \cdot F_A \qquad (85)$$

Where X is a dynamic radial load factor and Y is a dynamic axial load factor, which are given by the manufacturer of bearings. Subsequently the rating life $L_{10}$ - bearing life in millions of revolutions for 90 % reliability and $L_{10h}$ – bearing life in hours for 90 % reliability is determined, using equations below..

$$L_{10} = \left(\frac{C_d}{P}\right)^p \qquad (86)$$

$$L_{10h} = \left(\frac{C_d}{P}\right)^p \cdot \frac{10^6}{60 \cdot n} \qquad (87)$$

$C_d$ – Dynamic capacity of the bearing [N]

$p$ – Bearing coefficient, ball bearings $p = 3$, roller/needle bearings $p = 10/3$

$n$ – RPM of the shaft [RPM]

The real operating conditions are included in the modified rating life equation, where $a_1$ is a life adjustment factor for reliability, $a_{SKF}$ is SKF modification factor and $a_L$ is a life adjustment factor for the lubrication – given by the manufacturer of bearings [27].

$$L_{10mh} = a_1 \cdot a_{SKF} \cdot a_L \cdot L_{10h} \qquad (88)$$

Bearing life of individual bearings is listed in the table below, where $P_1$ is dynamic equivalent bearing load during duty cycle for bearings and $P_2$ is dynamic equivalent bearing load during duty cycle of maximal torque input. Gear support bearings are controlled statically against maximal static load. Eventual bearing life is a combination of both duty cycles and it is obtained using Ricardo s.r.o. SABR/Gear software.

| | $P_1$ [N] | $P_2$[N] | $C_d$ [N] | $L_{10}$ [mil rev] | $L_{10h}$ [h] | $L_{10mh}$ [h] |
|---|---|---|---|---|---|---|
| **HK 2210 left** | 169 | 232 | 7200 | 173337 | 722240 | 452824 |
| **HK 2210 middle** | 1129 | 3219 | 7200 | 369.6 | 1540.5 | 305.8 |
| **6305 ETN9** | 5966 | 13129 | 26000 | 205.8 | 857.5 | 343.8 |
| **6007 1st gear** | 252 | 353 | 16800 | 331.9 | 1383 | 780.1 |
| **6007 2nd gear** | 3225 | 6979 | | | | |
| **61907 1st gear** | 1048 | 3105 | 10800 | 402 | 1675 | 1046 |
| **61907 2nd gear** | 1629 | 4029 | | | | |
| **K43x48x27** | Max load = 13344 N | | | Calculated Safety Factor = 4.46 | | |
| **NJ206 1st gear** | 5293 | 13068 | 23500 | 867.8 | 3616 | 570 |
| **NJ206 2nd gear** | 2557 | 6355 | | | | |
| **SKF 306 1st gear** | 7853 | 17225 | 29700 | 301 | 1255 | 318.6 |
| **SKF 306 2nd gear** | 4196 | 9306 | | | | |
| **K35x40x27** | Max load = 8155 N | | | Calculated Safety Factor = 9.62 | | |
| **NU1011 1st gear** | 12621 | 31516 | 57200 | 3636 | 15153 | 1857 |
| **NU1011 2nd gear** | 6104 | 15250 | | | | |
| **6011 1st gear** | 9462 | 22644 | 29600 | 629 | 2621 | 370.9 |
| **6011 2nd gear** | 5310 | 11156 | | | | |

*Table 37 - Bearing life*

All used bearings met the required service life given by duty cycles discussed in the previous chapter 2.9.4.

## 2.9.11 SPLINE CALCULATION

Involute spline was chosen for the connection of following components:

- second synchronizer hub with the second input shaft,
- the second gear wheel with the output shaft,
- the first synchronizer hub with the output shaft,
- the inner clutch with the second input shaft
- the outer clutch with the first input shaft

The minimal active length $l'$ of the spline was determined using permissible pressure acting on the tooth flank $p_d = 120\ MPa$ and equation (89). Calculated values are listed in the Table 38.

$$l' > \frac{M_k}{0.5 \cdot m^2 \cdot z^2 \cdot \psi \cdot p_d} \tag{89}$$

m – Modulus [mm]

z – Number of teeth [-]

$\psi$ – Correction coefficient [-]

|  | Outer clutch | Inner clutch | 2nd synchro | 1st synchro | 1st wheel |
|---|---|---|---|---|---|
| Spline sign | 22x0.8x8f CSN 014952 | 35x0.8x8f CSN 014952 | 40x1x8f CSN 014952 | 40x1x8f CSN 014952 | 35x1x8f CSN 014952 |
| m [mm] | 0.8 | 0.8 | 1 | 1 | 1 |
| z [-] | 26 | 42 | 38 | 38 | 34 |
| $\psi$ [-] | 0.85 | 0.85 | 0.85 | 0.85 | 0.85 |
| l' [mm] | 11.33 | 4.34 | 3.39 | 9.78 | 12.22 |
| l [mm] | 20.5 | 10 | 13 | 14.1 | 18.4 |

*Table 38 - Spline dimensions*

After the design of the spline, the static strength control is performed. The Results are compared with the maximal allowable stress values. The tooth of the spline is loaded by:

- the bending moment which produces bending stress $\sigma$, $\sigma_D = 650\ MPa$ (90)
- the shear force that produces shear stress $\tau$, $\tau_D = 0.6\sigma_D = 390\ MPa$ (91)
- The pressure acting on the tooth flank $p$, $p_d = 200\ MPa$ (92)

$$\sigma = \frac{12 \cdot M_k \cdot h}{0.5 \cdot m \cdot l \cdot z^2 \cdot (2.17 \cdot m)^2} \leq \sigma_D \tag{90}$$

$$\tau = \frac{3 \cdot M_k}{0.5 \cdot m \cdot l \cdot z^2 \cdot 2.17 \cdot m} \leq \tau_D \tag{91}$$

$$p = \frac{2 \cdot M_k}{0.5 \cdot m^2 \cdot \psi \cdot z^2 \cdot l} \leq p_D \qquad (92)$$

For the spline strength control two load cases were applied. The first one is a "shock load", during which the maximal input torque of the motor is multiplied 1.5 times (coefficient for the dual clutch transmissions) in order to simulate eventual shock torque. The second one is reference duty cycle (Table 14) with the input torque of 100 Nm. To simulate the real life conditions, only 60 % of teeth transfer the torque in this case. The results are listed in the table below.

| | Outer clutch | Inner clutch | 2nd synchro | 1st synchro | 1st wheel |
|---|---|---|---|---|---|
| $\sigma_{shock}$ [MPa] | 484.87 | 406.77 | 229.08 | 486.84 | 582.51 |
| $\sigma_{reg}$ [MPa] | 359.16 | 301.31 | 169.69 | 360.62 | 431.49 |
| $\tau_{shock}$ [MPa] | 151.16 | 98.16 | 55.23 | 146.73 | 140.45 |
| $\tau_{reg}$ [MPa] | 86.6 | 72.71 | 40.91 | 108.69 | 104.04 |
| $p_{shock}$ [MPa] | 198.97 | 167.07 | 94.01 | 199.54 | 198.73 |
| $p_{reg}$ [MPa] | 147.39 | 123.76 | 69.64 | 180.98 | 177.07 |

*Table 39 – Static strength control of the spline*

All the splines used for the transfer of torque in the gearbox did not exceed stress limitations of the material.

## 2.9.12 GEARSHIFTING MECHANISM

In accordance with Figure 24, the gear change is performed by means of the radial dual clutch connected to the both input shafts and two single cone synchronizer packs connected to the first gear wheel and the second gear pinion. Due to this arrangement, the gear change occurs without the interruption of the power flow. The RPM of the motor for the upshift and the downshift that can be seen in Table 4, are fixed and chosen with regard to the optimal vehicle performance.

### 2.9.12.1 DUAL CLUTCH

For the connection of the motor output shaft and the transmission input shafts, the wet radially arranged dual clutch was utilized (Figure 44). The inner plate carrier of the inner clutch is connected to the second (hollow) input shaft. The inner plate carrier of the output clutch is connected to the first input shaft.
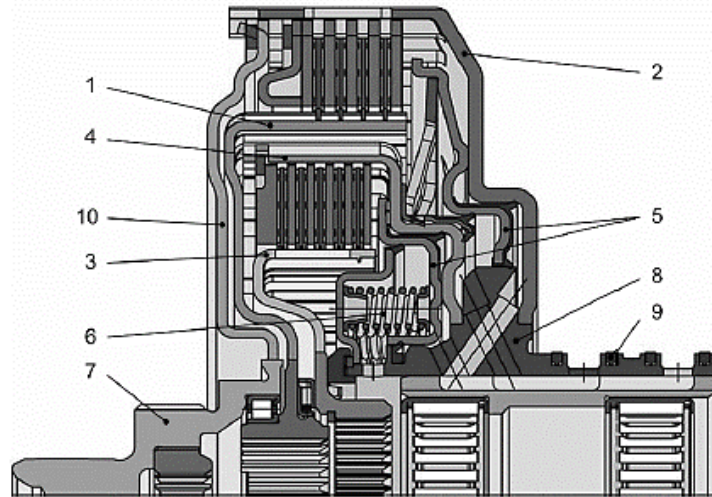
*Figure 44 - 1 Inner plate carrier of the outer clutch C1; 2 outer plate carrier of the outer clutch C1;3 inner plate carrier of the inner clutch C2; 4 outer plate carrier of the inner clutch C2; 5 piston; 6 compression spring; 7 input hub; 8 main hub; 9 sealing ring; 10 driving plate [20]*

### 2.9.12.2 DESIGN OF SYNCHRONIZERS

The function of synchronizer mechanism is to connect the desired idler gear with needle roller bearings with the gearbox shaft. The designed gearbox is equipped with two single cone synchronizer packs. The first pack is attached to the gearbox output shaft and it is engaging the first gear as can be seen in Figure 45 right. The second pack is attached to the second input shaft and its function is to engage second gear (Figure 45 left).
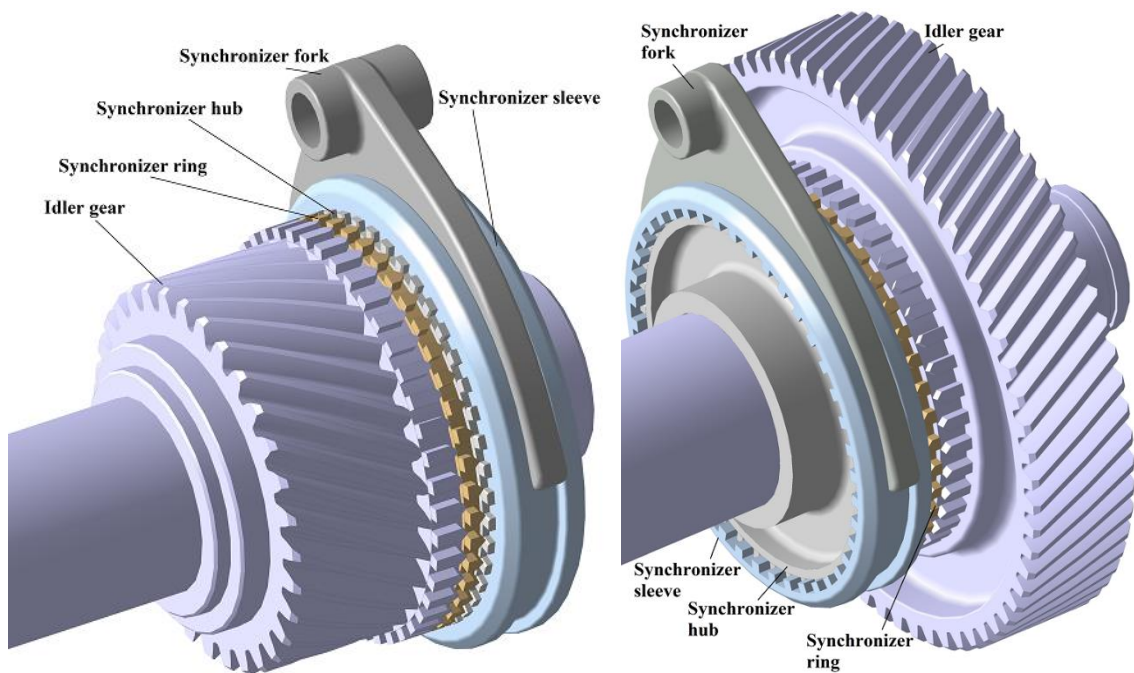


*Figure 45 – 2$^{nd}$ synchronizer pack (left), 1$^{st}$ synchronizer pack (right)*

Requirements for the synchronizer packs included maximal shifting force $F = 500\ N$ and maximal synchronization time $t = 0.3\ s$. The first proposal of the synchronizer dimensions was based on the required friction torque $T_R$ according to the equation (93). Dimensions of the synchronizers are listed in the Table 40.

$$T_R = j \cdot F \cdot \frac{d \cdot \mu}{2 \cdot \sin \alpha} \tag{93}$$

$j$ – Number of friction surfaces - 1 [-]

$d$ – Cone effective (mean) diameter [mm]

$\mu$ - coefficient of dynamic friction [-]

$\alpha$ – cone angle [°]

|  | 1st synchronizer pack | 2nd synchronizer pack |
|---|---|---|
| **d [mm]** | 68 | 57 |
| **$\mu$ [-]** | 0.13 | 0.13 |
| **$\alpha$ [°]** | 6.3 | 6.3 |
| **$d_{spline}$ [mm]** | 77 | 67 |

*Table 40 – Basic synchronizer dimensions*

Three shift cases can occur during gearbox operation:

- Shift from the "neutral" to first gear
- Shift from the first gear to the second gear
- Shift from the second gear to the first gear

The synchronization time of the proposed synchronizers, for the individual shifts was calculated from the shifting force using Ricardo SABR/Gear software and it is shown in the table below.

|  | Neutral to 1st | 1st to 2nd | 2nd to 1st |
|---|---|---|---|
| **$t_{syn}$ [s]** | 0 | 0.062 | 0.291 |

*Table 41 – Synchronization time*

## 2.9.13 DESIGN OF THE TRANSMISSION

After a series of calculation stated in previous chapters, the CAD model of the transmission was created using Catia V5 CAD software. The created model provides insight to the gearbox construction. It is not used for further calculation or strength control. The Attachment 3 includes a cross-sectional drawing of the gearbox CAD model.

### 2.9.13.1 INPUT SHAFTS

An input shaft configuration is depicted in Figure 46. The first input shaft is fitted with the built in first gear pinion. It is fixed in the 2 needle bearings (retained by circlips) connected to the second input shaft and the ball bearing on the right that is attached to the housing located in the gearbox casing and screwed by the cap. The second input shaft is fitted with the second gear pinion rotating on the needle bearing and the second synchronizer pack connected to the shaft via involute spline. The shaft is fixed in 2 ball bearings attached to the housings in the gearbox casing.
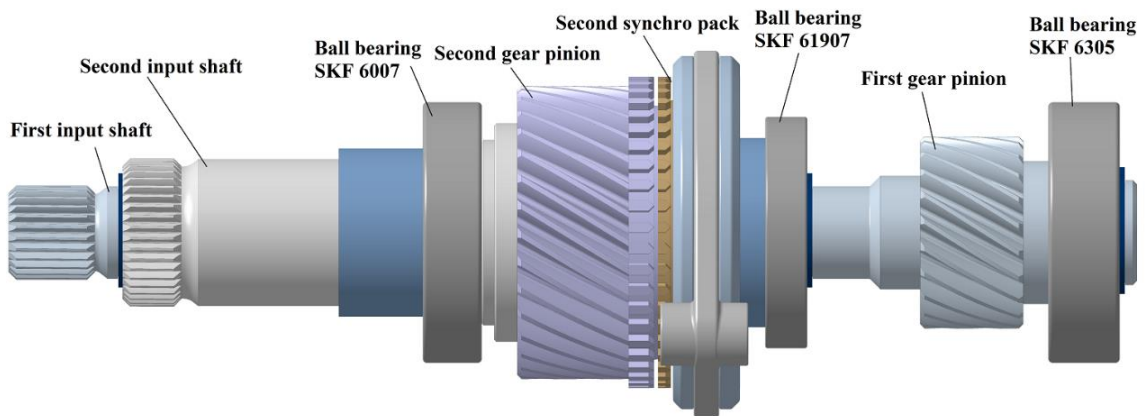


*Figure 46 – Input shafts*

### 2.9.13.2 COUNTERSHAFT (OUTPUT) SHAFT

The output shaft is fitted with the second gear wheel connected to it via involute spline, built in final drive pinion, the first synchronizer pack and the first gear wheel rotating on the needle bearings as can be seen in Figure 47. The shaft is rotating in the roller bearing attached to the housing in the gearbox casing on the left side and in the ball bearing attached to the housing and screwed by the cap.
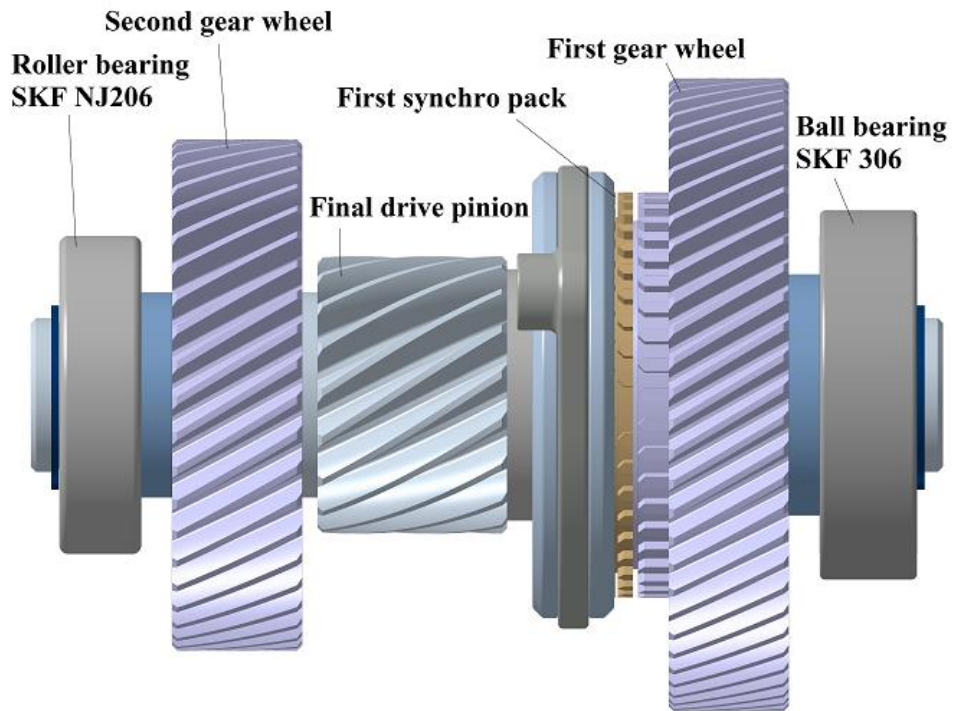
*Figure 47 – Output shaft*

### 2.9.13.3  TRASNMISSION ASSEMBLY

Transmission assembly together with the final drive is shown in the figure below.
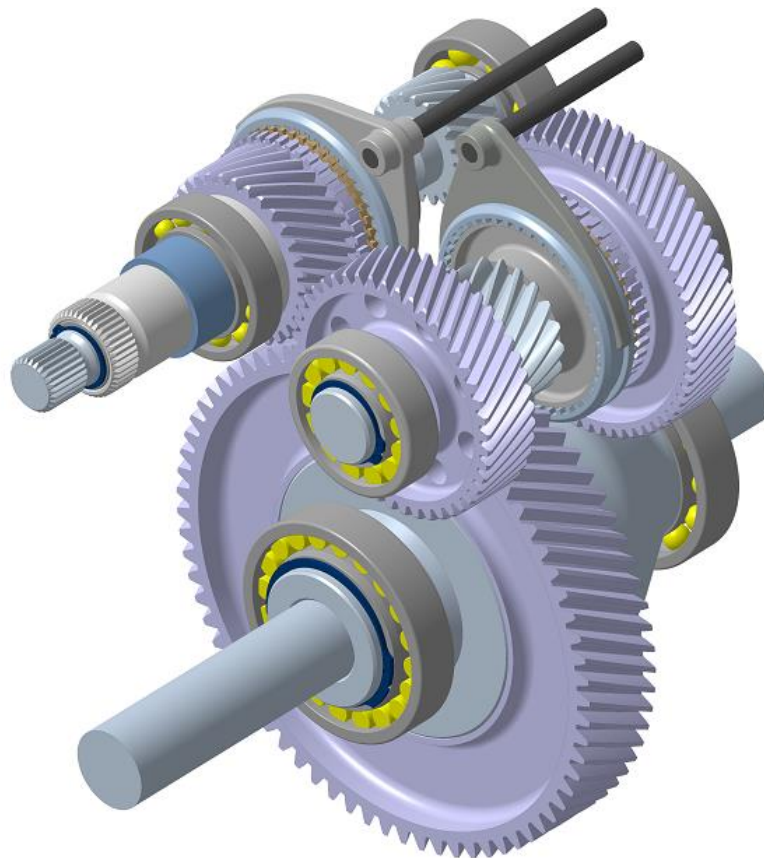


*Figure 48 – Transmission assembly*

#### 2.9.13.4  TRANSMISSION CASING

The transmission assembly is placed in the aluminum alloy (AlSi7Mg) casing, composed of two parts screwed together by 10 hexagon head bolts (DIN 6921) as can be seen in the figures below. The casing is connected to the electric motor by 8 bolts (DIN 6921) located in the flange which as well provides room for the dual clutch assembly. On the opposite side, there is the casing cap in order to provide easy installation and retaining of the shaft bearings and the mount for the shifting mechanism. From above, the casing is attached to the frame of the vehicle.
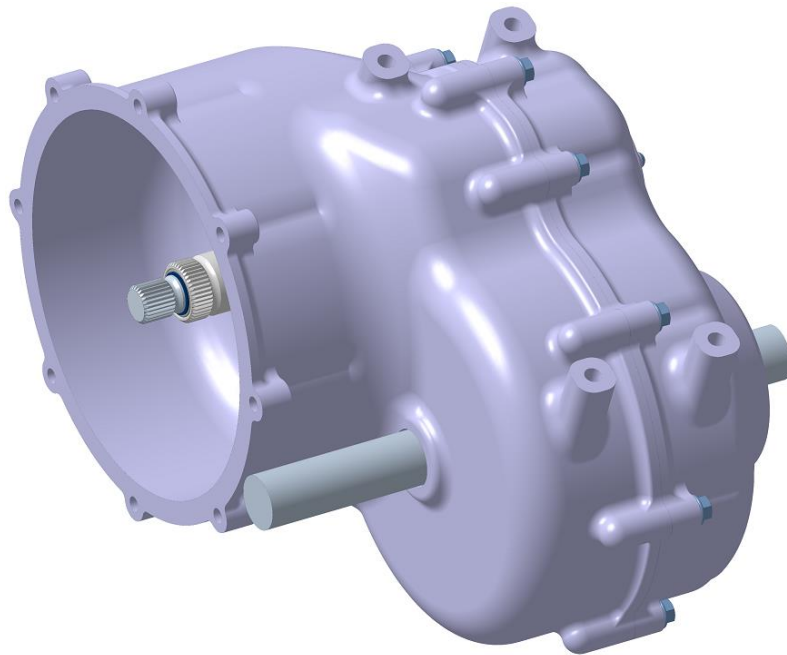


*Figure 49 – Transmission casing – isometric view*
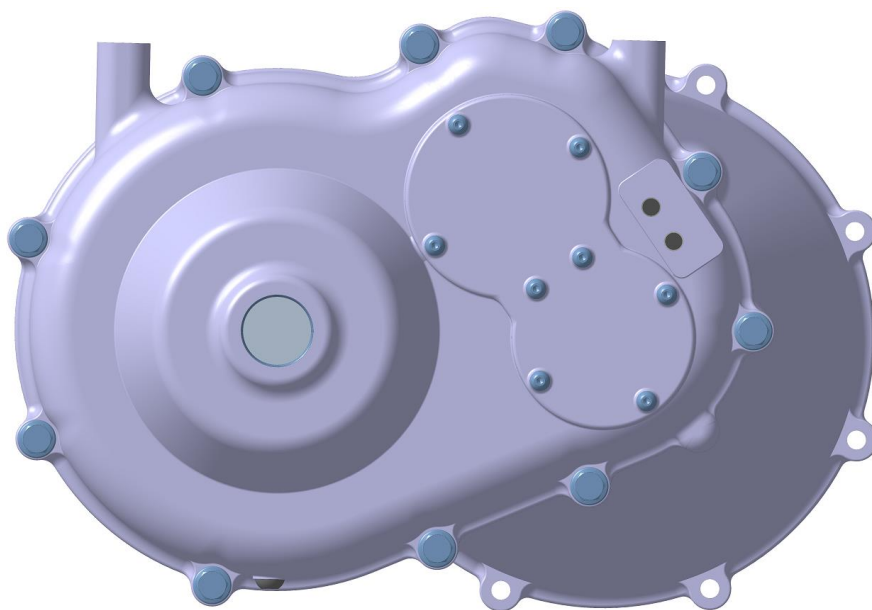


*Figure 50 – Transmission casing – side view*

# CONCLUSION

The main goal of this thesis was to design a multi-speed layshaft gearbox for a passenger electric vehicle. The thesis was divided into two main parts. In the first part, research about gearboxes in the currently available electric vehicles was conducted in order to find the state of art gearbox types. The results of the research indicate that the majority of EV manufacturers equip their vehicles with a single speed gearbox (with the exception of Porsche Taycan).

After research, the vehicle parameters were selected and the specifications of the Chevrolet Bolt EV were used. The layout where the electric motor with the gearbox are mounted transversely in the front of the vehicle was chosen for the procedure. This powertrain configuration is suitable for single and multi-speed gearboxes. According to the power requirements, three traction motors (130 kW, 120 kW, 115 kW) paired with 3 gearboxes (preliminary gear ratios) were used for software simulation.

The software simulation of driving consisted of the 5 test procedures – acceleration, top speed, uphill ride, highway driving and WLTC. Thanks to the multi speed gearbox, the vehicle can be powered by an electric motor with a lower power output then the motor in the single speed one. After a review of the energy consumption data, it can be summarized that adding one more gear to the fixed gear gearbox reduces the average consumption up to 3.8 % on the highway. On the other hand, the use of three speed gearbox reduces consumption by only 0.5 - 0.8 % compared to the 2 speed gearbox. By taking into account energy consumption, weight and acquisition costs, the most suitable gearbox for the chosen vehicle is the two speed dual clutch gearbox.

The proposal process started by dividing the total gear ratio between the final drive and the gearbox. After choosing the suitable number of teeth for every gear pair, the basic gear geometry was calculated. Afterwards the shaft dimensioning together with the bearing selection and spline proposal was done. For the determination of the service life, the duty cycle corresponding with the usage of this type of gearbox was created. It comprises of 4 cases – gear bending, gear surface, bearings and maximal torque input.

Subsequently, the basic strength calculations – gear load capacity (bending and contact stress), shaft strength control, bearing life calculation and spline control was carried out using Ricardo SABR/Gear software. The results indicate that every component meets the requirements.

For visualization purposes, the CAD model of the gearbox that involves an internal gear mechanism and gearbox casing was created. The model is supplemented with a production drawing of the output shaft (Attachment 2) and a cross-sectional drawing of the gearbox (Attachment 3).

In conclusion, all of the set tasks of this diploma thesis were fulfilled. Other improvements of the proposed gearbox such as optimization of the shifting mechanism or gearbox casing strength control were suggested for future work.

# REFERENCES

[1]     Chevrolet Bolt EV deep look on drive unit. *EVNewsTopic* [online]. 2019 [2020-10-06]. Available from: https://www.evnewstopic.com/2019/03/chevrolet-bolt-ev-deep-look-on-drive.html

[2]     Volkswagen e-Golf and e-Up! Electric Cars 2013 [online]. 2013 [2020-06-09]. Available from: http://www.autoconcept-reviews.com/cars_reviews/volkswagen/Volkswagen-e-golf-and-e-up-electric-cars-2013/wallpapers/9%20-%20Volkswagen%20e-up.jpg

[3]     Hillier, V.A.W. (2001). "Planetary gearing and unidirectional clutches". Fundamentals of Motor Vehicle Technology (4th ed.). Cheltenham, UK: Nelson Thornes. p. 244. ISBN 0-74-870531-7.

[4]     VLK, František. *Převody motorových vozidel: Spojky Převodovky Rozvodovky Diferenciály Hnací hřídele Klouby.* Brno: Prof. Ing. František Vlk, DrSc., nakladatelství a vydavatelství, 2006, 371 s. : il. ISBN80-239-6463-1

[5]     Audi e-tron defined. EVSpecifications [online]. 2019 [2020-06-09]. Available from: https://www.evspecifications.com/en/news/b86423

[6]     PARKINSON, Rob. Modular, Multi-speed electric vehicle drive units. *Ricardo UK Ltd.,.* United Kingdom, 2019

[7]     TRACY, David. An Extremely Detailed Look At The Porsche Taycan's Engineering Designed To Take On Tesla. 2019. [2020-06-09] Available from: https://jalopnik.com/an-extremely-detailed-look-at-the-porsche-taycans-engin-1837802533

[8]     MASUZAVA, Toru. Motor design and impeller suspension. Mechanical Circulatory and Respiratory Support [online]. 2018 [2020-07-14]. Available from: https://www.sciencedirect.com/topics/engineering/motor-efficiency

[9]     GKN Electric Motor and Generator Technology. Ricardo UK Ltd., United Kingdom, 2014.

[10]   Permanent Magnet Synchronous Motor (PMSM): [online]. 2017 [2020-07-14]. Available from: https://alliedmarketresearch.wordpress.com/2017/02/03/permanent-magnet-synchronous-motor-pmsm-market-is-expected-to-garner-31-1-billion-globally-by-2022/

[11] Permanent Magnet Synchronous Motor (PMSM): PMSM Control [online]. 2015 [2020-07-15]. Available from: http://www.microchip.com/design-centers/motor-control-and-drive/motor-types/pmsm

[12] AC Induction Motor (ACIM): ACIM Control. [online]. 2014 [2020-07-16]. Available from: http://www.microchip.com/design-centers/motor-control-and-drive/motor-types/acim

[13] GT-SUITE Overview: From Concept Design to Detailed System Analysis. GTiSoft [online]. USA, 2019 [2020-07-16]. Available from: https://www.gtisoft.com/gt-suite/gt-suite-overview/

[14] Worldwide Harmonized Light Vehicles Test Cycle (WLTC). *DieselNet* [online]. Canada: Ecopoint, 2019 [2020-07-16]. Available from: https://dieselnet.com/standards/cycles/wltp.php

[15] Emission test cycles. *Dieselnet* [online]. Canada: Ecopoint, 2019 [2020-08-27]. Available from: https://dieselnet.com/standards/cycles/ece_eudc.php

[16] Federal Test Procedure (FTP). *Dieselnet* [online]. Canada: Ecopoint, 2019 [2020-08-27]. Available from: https://dieselnet.com/standards/cycles/ftp75.php

[17] EPA Highway Fuel Economy Test Cycle (HWFET). *Dieselnet* [online]. Canada: Ecopoint, 2019 [2020-08-27]. Available from: https://dieselnet.com/standards/cycles/hwfet.php

[18] C.J. Tragakis. Longitudinal vs Transverse Engines. *CJPonyParts* [online]. Harrisburg, May 14, 2020 [2020-08-27]. Available from: https://www.cjponyparts.com/resources/longitudinal-vs-transverse-engines

[19] LIMA, Pedro. *PUSHEVS* [online]. 2018 [2020-09-22]. Available from: https://pushevs.com/2018/06/27/chevrolet-bolt-ev-vs-hyundai-kona-electric/

[20] NAUNHEIMER, Herald. Automotive transmissions: Fundamentals, Selection, Design and Application. Second edition. Germany: Springer, 2011. ISBN 978-3-642-16213-8.

[21] NICA, Gabriel. How It's Made: BMW i3 Gearbox. *Autoevolution* [online]. 2014 [2020-10-09]. Available from: https://www.autoevolution.com/news/how-its-made-bmw-i3-gearbox-video-76174.html#

[22] HANLEY, Steve. Tesla Model 3 Motor & Gearbox Survive 1 Million Miles Of Testing. CleanTechnica [online]. USA, 2018 [2020-10-09]. Available from: https://cleantechnica.com/2018/10/16/tesla-model-3-motor-gearbox-survive-1-million-miles-of-testing/

[23]    List of electric cars currently available. Wikipedia [online]. 2020 [2020-10-09]. Available from:

https://en.wikipedia.org/wiki/List_of_electric_cars_currently_available

[24]    MURPHY, Jim. What's the Difference Between AC Induction, Permanent Magnet, and Servomotor Technologies? *MachineDesign* [online]. 2012 [2020-10-12]. Available from: https://www.machinedesign.com/motors-drives/article/21831709/whats-the-difference-between-ac-induction-permanent-magnet-and-servomotor-technologies

[25]    KUNANOPPADOL, Jarut. The Concept to Measure the Overall Car Performance [online]. Thailand, 2012 [2020-10-19]. Available from: https://www.researchgate.net/publication/277830894_The_Concept_to_Measure_the_Overall_Car_Performance. Silpakorn University.

[26]    SHIGLEY, Joseph Edward, Charles R. MISCHKE a Richard G. BUDYNAS, VLK, Miloš, *Konstruování strojních součástí.* V Brně: VUTIUM, 2010. ISBN 978-80-214-2629-0

[27]    SKF GROUP. *Rolling Bearings: Deep Groove Ball Bearings* [online]. 2016 [2020- 05-24]. Available from: http://www.skf.com/binary/77-121486/SKF-rolling-bearings-catalogue.pdf

# LIST OF FIGURES

# LIST OF TABLES

# ATTACHMENTS

Attachment 1 – Gear load capacity calculation

Attachment 2 – Production drawing of the gearbox output shaft

Attachment 3 – Cross-sectional drawing of the gearbox

# ATTACHMENT 1

1st gear pair load capacity calculation:

## ISO contact stress:

| ISO CONTACT STRESS DATA | pinion | | wheel |
|---|---|---|---|
| ISO Zone Factor - ZH | | 2.174 | |
| ISO Elasticity Factor - ZE | | 189.812 | |
| ISO Contact Ratio Factor - Zε | | 0.861 | |
| ISO Helix Angle Factor - Zβ | | 1.075 | |
| ISO Life Factor - ZNT | 1.298 | | 1.407 |
| ISO Viscosity Factor - ZL | 0.996 | | 0.998 |
| ISO Velocity Factor - ZV | 0.998 | | 0.999 |
| ISO Roughness Factor - ZR | 0.954 | | 0.971 |
| ISO Complex Lubrication Factor - ZVZLZR | 0.949 | | 0.968 |
| ISO Single Pair Contact Factors - ZB,ZD | 1.000 | | 1.000 |
| ISO Hardening Factor - ZW | 1.000 | | 1.000 |
| ISO Face Load Factor KHβ | | 1.126 | |
| ISO Transverse Load Factor KHα | | 1.333 | |
| ISO Running-in Allowance - yα (microns) | | 1.200 | |
| ISO Running-in Allowance - yβ (microns) | | 0.766 | |

| CONTACT | pinion | | wheel | |
|---|---|---|---|---|
| ISO Cont. Endur. Limit σHlim | 1500.000 | MPa | 1500.000 | MPa |
| ISO Limit Contact Stress σHG | 1846.619 | MPa | 2043.182 | MPa |
| ISO Permissible Stress σHP | 1846.619 | MPa | 2043.182 | MPa |
| ISO Nom. Contact Stress σHO | 1008.377 | MPa | | |
| ISO Actual Contact Stress σH | 1283.031 | MPa | 1283.031 | MPa |
| ISO Contact Life | 708.893 | hour | 2062.235 | hour |
| ISO Contact Damage | 0.935 | % | 0.321 | % |
| ISO Safety Factor SH | 1.439 | | 1.592 | |

## ISO bending stress:

| ISO BENDING STRESS PARAMETERS | pinion | | wheel |
|---|---|---|---|
| ISO Minimum Safety Factor - SFmin | | 1.000 | |
| ISO Correction Factor - YST | | 2.000 | |
| ISO Contact Ratio Factor - Yε | | 0.683 | |
| ISO Helix Factor - Yβ | | 0.750 | |
| ISO Size Factor - YX | | 1.000 | |
| ISO Size Factor - YX ref. | 1.000 | | 1.000 |
| ISO Radius of Root Fillet - ρF/mn | 0.601 | | 0.495 |
| ISO Tooth-root Normal Chord - rootChord | 2.119 | | 2.283 |
| ISO Bending Moment Arm - hFe/mn | 1.013 | | 0.915 |
| ISO Form Factor - YF | 1.366 | | 1.048 |
| ISO Correction Factor - YS | 1.883 | | 2.256 |
| ISO Rim Thickness Factor - YB | 1.000 | | 1.000 |
| ISO Notch Parameter - qs | 1.765 | | 2.306 |
| ISO Life Factor - YNT | 1.207 | | 1.364 |
| ISO Load Factor - KFβ | | 1.106 | |
| ISO Load Factor - KFα | | 1.333 | |
| ISO Running-in Allowance - yα (microns) | | 1.200 | |
| ISO Running-in Allowance - yβ (microns) | | 0.766 | |
| ISO Surface Factor - YRrT | 0.968 | | 0.973 |
| ISO Sensitivity Factor YDrT | 0.983 | | 1.035 |

| BENDING | pinion | | wheel | |
|---|---|---|---|---|
| ISO Nominal Stress σFlim | 460.000 | MPa | 460.000 | MPa |
| ISO Allowable Stress σFE | 920.000 | MPa | 920.000 | MPa |
| ISO Root Limit Stress σFG | 1056.426 | MPa | 1263.947 | MPa |
| ISO Permissible Stress σFP | 1056.426 | MPa | 1263.947 | MPa |
| ISO Nom. Bending Stress σFO | 242.078 | MPa | 232.997 | MPa |
| ISO Actual Bending Stress σF | 384.966 | MPa | 370.525 | MPa |
| ISO Bending Life | INFINITE | hour | INFINITE | hour |
| ISO Bending Damage | 0.000 | % | 0.000 | % |
| ISO Safety Factor SF | 2.744 | | 3.411 | |

## 2nd gear pair load capacity calculation:

## ISO contact stress:

| ISO CONTACT STRESS DATA | pinion | | wheel |
|---|---|---|---|
| ISO Zone Factor - ZH | | 2.225 | |
| ISO Elasticity Factor - ZE | | 189.812 | |
| ISO Contact Ratio Factor - Zε | | 0.848 | |
| ISO Helix Angle Factor - Zβ | | 1.075 | |
| ISO Life Factor - ZNT | 1.217 | | 1.249 |
| ISO Viscosity Factor - ZL | 0.995 | | 0.996 |
| ISO Velocity Factor - ZV | 1.006 | | 1.005 |
| ISO Roughness Factor - ZR | 0.943 | | 0.948 |
| ISO Complex Lubrication Factor - ZVZLZR | 0.944 | | 0.949 |
| ISO Single Pair Contact Factors - ZB,ZD | 1.000 | | 1.000 |
| ISO Hardening Factor - ZW | 1.000 | | 1.000 |
| ISO Face Load Factor KHβ | | 1.004 | |
| ISO Transverse Load Factor KHα | | 1.654 | |
| ISO Running-in Allowance - yα (microns) | | 1.200 | |
| ISO Running-in Allowance - yβ (microns) | | 0.016 | |

| CONTACT | pinion | | wheel | |
|---|---|---|---|---|
| ISO Cont. Endur. Limit σHlim | 1500.000 | MPa | 1500.000 | MPa |
| ISO Limit Contact Stress σHG | 1723.131 | MPa | 1777.813 | MPa |
| ISO Permissible Stress σHP | 1723.131 | MPa | 1777.813 | MPa |
| ISO Nom. Contact Stress σHO | | 673.354 | MPa | |
| ISO Actual Contact Stress σH | 982.493 | MPa | 982.493 | MPa |
| ISO Contact Life | INFINITE | hour | INFINITE | hour |
| ISO Contact Damage | 0.000 | % | 0.000 | % |
| ISO Safety Factor SH | 1.754 | | 1.809 | |

## ISO bending stress

| ISO BENDING STRESS PARAMETERS | pinion | | wheel |
|---|---|---|---|
| ISO Minimum Safety Factor - SFmin | | 1.000 | |
| ISO Correction Factor - YST | | 2.000 | |
| ISO Contact Ratio Factor - Yε | | 0.671 | |
| ISO Helix Factor - Yβ | | 0.750 | |
| ISO Size Factor - YX | | 1.000 | |
| ISO Size Factor - YX ref. | 1.000 | | 1.000 |
| ISO Radius of Root Fillet - ρF/mn | 0.591 | | 0.565 |
| ISO Tooth-root Normal Chord - rootChord | 2.132 | | 2.204 |
| ISO Bending Moment Arm - hFe/mn | 0.803 | | 0.895 |
| ISO Form Factor - YF | 1.069 | | 1.111 |
| ISO Correction Factor - YS | 2.051 | | 2.076 |
| ISO Rim Thickness Factor - YB | 1.000 | | 1.000 |
| ISO Notch Parameter - qs | 1.802 | | 1.951 |
| ISO Life Factor - YNT | 1.023 | | 1.064 |
| ISO Load Factor - KFβ | | 1.003 | |
| ISO Load Factor - KFα | | 1.654 | |
| ISO Running-in Allowance - yα (microns) | | 1.200 | |
| ISO Running-in Allowance - yβ (microns) | | 0.016 | |
| ISO Surface Factor - YRrT | 0.961 | | 0.962 |
| ISO Sensitivity Factor YDrT | 0.994 | | 0.997 |

| BENDING | pinion | | wheel | |
|---|---|---|---|---|
| ISO Nominal Stress σFlim | 460.000 | MPa | 460.000 | MPa |
| ISO Allowable Stress σFE | 920.000 | MPa | 920.000 | MPa |
| ISO Root Limit Stress σFG | 898.271 | MPa | 938.885 | MPa |
| ISO Permissible Stress σFP | 898.271 | MPa | 938.885 | MPa |
| ISO Nom. Bending Stress σFO | 103.666 | MPa | 113.794 | MPa |
| ISO Actual Bending Stress σF | 220.559 | MPa | 242.107 | MPa |
| ISO Bending Life | INFINITE | hour | INFINITE | hour |
| ISO Bending Damage | 0.000 | % | 0.000 | % |
| ISO Safety Factor SF | 4.073 | | 3.878 | |

Final drive gear pair load capacity calculation:

ISO contact stress:

The first gear engaged:

**ISO CONTACT STRESS DATA**

| | pinion | | wheel |
|---|---|---|---|
| ISO Zone Factor - ZH | | 2.258 | |
| ISO Elasticity Factor - ZE | | 189.812 | |
| ISO Contact Ratio Factor - Zε | | 0.851 | |
| ISO Helix Angle Factor - Zβ | | 1.075 | |
| ISO Life Factor - ZNT | 1.407 | | 1.566 |
| ISO Viscosity Factor - ZL | 0.998 | | 1.000 |
| ISO Velocity Factor - ZV | 0.993 | | 0.999 |
| ISO Roughness Factor - ZR | 0.973 | | 0.995 |
| ISO Complex Lubrication Factor - ZVZLZR | 0.964 | | 0.994 |
| ISO Single Pair Contact Factors - ZB,ZD | 1.000 | | 1.000 |
| ISO Hardening Factor - ZW | 1.000 | | 1.000 |
| ISO Face Load Factor KHβ | | 1.000 | |
| ISO Transverse Load Factor KHα | | 1.257 | |
| ISO Running-in Allowance - yα (microns) | | 1.350 | |
| ISO Running-in Allowance - yβ (microns) | | 0.000 | |

| CONTACT | pinion | | wheel | |
|---|---|---|---|---|
| ISO Cont. Endur. Limit σHlim | 1500.000 | MPa | 1500.000 | MPa |
| ISO Limit Contact Stress σHG | 2033.400 | MPa | 2333.841 | MPa |
| ISO Permissible Stress σHP | 2033.400 | MPa | 2333.841 | MPa |
| ISO Nom. Contact Stress σHO | | 1141.001 MPa | | |
| ISO Actual Contact Stress σH | 1291.103 | MPa | 1291.103 | MPa |
| ISO Contact Life | 980.533 | hour | 4037.489 | hour |
| ISO Contact Damage | 0.676 | % | 0.164 | % |
| ISO Safety Factor SH | 1.575 | | 1.808 | |

The second gear engaged:

**ISO CONTACT STRESS DATA**

| | pinion | | wheel |
|---|---|---|---|
| ISO Zone Factor - ZH | | 2.258 | |
| ISO Elasticity Factor - ZE | | 189.812 | |
| ISO Contact Ratio Factor - Zε | | 0.851 | |
| ISO Helix Angle Factor - Zβ | | 1.075 | |
| ISO Life Factor - ZNT | 1.249 | | 1.390 |
| ISO Viscosity Factor - ZL | 0.996 | | 0.998 |
| ISO Velocity Factor - ZV | 0.995 | | 0.997 |
| ISO Roughness Factor - ZR | 0.948 | | 0.970 |
| ISO Complex Lubrication Factor - ZVZLZR | 0.940 | | 0.965 |
| ISO Single Pair Contact Factors - ZB,ZD | 1.000 | | 1.000 |
| ISO Hardening Factor - ZW | 1.000 | | 1.000 |
| ISO Face Load Factor KHβ | | 1.000 | |
| ISO Transverse Load Factor KHα | | 1.597 | |
| ISO Running-in Allowance - yα (microns) | | 1.350 | |
| ISO Running-in Allowance - yβ (microns) | | 0.000 | |

| CONTACT | pinion | | wheel | |
|---|---|---|---|---|
| ISO Cont. Endur. Limit σHlim | 1500.000 | MPa | 1500.000 | MPa |
| ISO Limit Contact Stress σHG | 1760.971 | MPa | 2013.323 | MPa |
| ISO Permissible Stress σHP | 1760.971 | MPa | 2013.323 | MPa |
| ISO Nom. Contact Stress σHO | | 795.676 MPa | | |
| ISO Actual Contact Stress σH | 1041.566 | MPa | 1041.566 | MPa |
| ISO Contact Life | INFINITE | hour | INFINITE | hour |
| ISO Contact Damage | 0.000 | % | 0.000 | % |
| ISO Safety Factor SH | 1.691 | | 1.933 | |

## ISO bending stress:

**ISO BENDING STRESS PARAMETERS**

| | pinion | | wheel |
|---|---|---|---|
| ISO Minimum Safety Factor - SFmin | | 1.000 | |
| ISO Correction Factor - YST | | 2.000 | |
| ISO Contact Ratio Factor - Yε | | 0.673 | |
| ISO Helix Factor - Yβ | | 0.750 | |
| ISO Size Factor - YX | | 1.000 | |
| ISO Size Factor - YX ref. | 1.000 | | 1.000 |
| ISO Radius of Root Fillet - ρF/mn | 0.619 | | 0.581 |
| ISO Tooth-root Normal Chord - rootChord | 2.031 | | 2.207 |
| ISO Bending Moment Arm - hFe/mn | 0.861 | | 0.941 |
| ISO Form Factor - YF | 1.275 | | 1.166 |
| ISO Correction Factor - YS | 1.890 | | 2.016 |
| ISO Rim Thickness Factor - YB | 1.000 | | 1.000 |
| ISO Notch Parameter - qs | 1.642 | | 1.898 |

## The first gear engaged:

**ISO BENDING STRESS DATA**

| | pinion | | wheel |
|---|---|---|---|
| ISO Life Factor - YNT | 1.363 | | 1.603 |
| ISO Load Factor - KFβ | | 1.000 | |
| ISO Load Factor - KFα | | 1.257 | |
| ISO Running-in Allowance - yα (microns) | | 1.350 | |
| ISO Running-in Allowance - yβ (microns) | | 0.000 | |
| ISO Surface Factor - YRrT | 0.973 | | 0.980 |
| ISO Sensitivity Factor YDrT | 0.978 | | 1.001 |

| BENDING | pinion | | wheel | |
|---|---|---|---|---|
| ISO Nominal Stress σFlim | 460.000 | MPa | 460.000 | MPa |
| ISO Allowable Stress σFE | 920.000 | MPa | 920.000 | MPa |
| ISO Root Limit Stress σFG | 1192.974 | MPa | 1446.353 | MPa |
| ISO Permissible Stress σFP | 1192.974 | MPa | 1446.353 | MPa |
| ISO Nom. Bending Stress σFO | 231.024 | MPa | 236.112 | MPa |
| ISO Actual Bending Stress σF | 295.806 | MPa | 302.321 | MPa |
| ISO Bending Life | INFINITE | hour | INFINITE | hour |
| ISO Bending Damage | 0.000 | % | 0.000 | % |
| ISO Safety Factor SF | 4.033 | | 4.784 | |

## The second gear engaged:

**ISO BENDING STRESS DATA**

| | pinion | | wheel |
|---|---|---|---|
| ISO Life Factor - YNT | 1.064 | | 1.251 |
| ISO Load Factor - KFβ | | 1.000 | |
| ISO Load Factor - KFα | | 1.597 | |
| ISO Running-in Allowance - yα (microns) | | 1.350 | |
| ISO Running-in Allowance - yβ (microns) | | 0.000 | |
| ISO Surface Factor - YRrT | 0.962 | | 0.969 |
| ISO Sensitivity Factor YDrT | 0.988 | | 0.997 |

| BENDING | pinion | | wheel | |
|---|---|---|---|---|
| ISO Nominal Stress σFlim | 460.000 | MPa | 460.000 | MPa |
| ISO Allowable Stress σFE | 920.000 | MPa | 920.000 | MPa |
| ISO Root Limit Stress σFG | 931.064 | MPa | 1112.507 | MPa |
| ISO Permissible Stress σFP | 931.064 | MPa | 1112.507 | MPa |
| ISO Nom. Bending Stress σFO | 112.346 | MPa | 114.820 | MPa |
| ISO Actual Bending Stress σF | 192.512 | MPa | 196.753 | MPa |
| ISO Bending Life | INFINITE | hour | INFINITE | hour |
| ISO Bending Damage | 0.000 | % | 0.000 | % |
| ISO Safety Factor SF | 4.836 | | 5.654 | |